© 2021. Published by The Company of Biologists Ltd | Development (2021) 148, dev199630. doi:10.1242/dev.199630

STEM CELLS AND REGENERATION

RESEARCH ARTICLE

Distinct roles of Bendless in regulating FSC niche competition and daughter cell differentiation

Sumitra Tatapudy, Jobelle Peralta and Todd Nystul*

ABSTRACT

A major goal in the study of adult stem cells is to understand how cell fates are specified at the proper time and place to facilitate tissue homeostasis. Here, we found that an E2 ubiquitin ligase, Bendless (Ben), has multiple roles in the *Drosophila* ovarian epithelial follicle stem cell (FSC) lineage. First, Ben is part of the JNK signaling pathway, and we found that it, as well as other JNK pathway genes, are essential for differentiation of FSC daughter cells. Our data suggest that JNK signaling promotes differentiation by suppressing the activation of the EGFR effector, ERK. Also, we found that loss of *ben*, but not the JNK kinase *hemipterous*, resulted in an upregulation of hedgehog signaling, increased proliferation and increased niche competition. Lastly, we demonstrate that the hypercompetition phenotype caused by loss of *ben* is suppressed by decreasing the rate of proliferation or knockdown of the hedgehog pathway effector, Smoothened (Smo). Taken together, our findings reveal a new layer of regulation in which a single gene influences cell signaling at multiple stages of differentiation in the early FSC lineage.

KEY WORDS: *Drosophila*, Hedgehog, JNK, Notch, Epithelial stem cell, Follicle epithelium

INTRODUCTION

A defining feature of adult stem cells is the ability to self-renew while producing daughters that differentiate into functional cell types in the tissue. This segregation of stem cell and daughter cell fates requires the coordinated action of multiple self-renewal and differentiation signals to ensure that each cell acquires the proper fate. It is likely that newly produced daughter cells need to both reduce response to niche signals and upregulate differentiation cues to differentiate properly, but how the transition from a stem cell identity to a differentiating daughter cell identity is regulated is not well-understood.

The follicle epithelium of the *Drosophila* ovary is a tractable model for studying the mechanisms that govern cell fate transitions in an epithelial stem cell lineage (Rust and Nystul, 2020). The *Drosophila* ovary is made up of approximately 16 strands of developing follicles called ovarioles (Miller, 1950). Follicle production begins at the anterior tip of the ovariole in a structure called the germarium, which is divided into four regions based on the stages of germ cell development. New germ cells are produced by germline stem cells in Region 1 and undergo four rounds of synchronous division to become a 16-cell cyst of interconnected cells as they move into Region 2a (Carpenter, 1975; Koch and King, 1966). Germ cells then encounter the follicle epithelium at the border between Regions 2a and 2b, where the follcile stem cells (FSCs) reside. FSCs produce a transit amplifying population of cells called pre-follicle cells (pFCs), which associate with germ cells as they enter Region 2b and begin to differentiate into one of three main cell types: polar cells, stalk cells or main body follicle cells (Fig. 1A).

FSCs self-renewal is controlled by several signaling pathways, including EGFR, Wnt and Hedgehog (Hh), which are active in the FSCs and must be downregulated in newly-produced pFCs for differentiation to occur (Castanieto et al., 2014; Hartman et al., 2013; Huang and Kalderon, 2014; Johnston et al., 2016; Kim-Yip and Nystul, 2018; Melamed and Kalderon, 2020; Sahai-Hernandez and Nystul, 2013; Singh et al., 2018; Song and Xie, 2003; Zhang and Kalderon, 2000, 2001). In pFCs, activation of Notch signaling in response to a Delta signal from germ cells initiates differentiation toward the polar cell fate (Dai et al., 2017; Lopez-Schier and St Johnston, 2001; Nystul and Spradling, 2010). Polar cells activate JAK/STAT signaling in neighboring cells, inducing a stalk cell fate, and the pFCs that do not become polar or stalk cells differentiate into main body follicle cells (Assa-Kunik et al., 2007; Dai et al., 2017). FSCs commonly divide with asymmetric outcomes to self-renew and produce a pFC, but can also divide symmetrically, for example, during FSC loss and replacement events (Kronen et al., 2014; Margolis and Spradling, 1995; Wang et al., 2012). This suggests that the fate of the FSC daughter cells is not specified at the time of division, but the regulation of these decisions is not fully understood. One strategy to understand the regulation of these cell fate decisions has been to identify mutations that affect the rate of FSC loss and replacement by conferring a competitive advantage or disadvantage for niche occupancy (Cook et al., 2017; Kronen et al., 2014; Wang et al., 2012): these mutant phenotypes are referred to as hypercompetition and hypocompetition, respectively. Recently, we reported the results of a forward genetic screen for FSC niche mutants (Cook et al., 2017). Among the strongest hits from the screen was an allele of *bendless* (*ben*), which is an E2 ubiquitin ligase that is a core component of the JNK pathway (Ma et al., 2014). The allele ben^{A} contains a single nonsense mutation in the C-terminal domain of the protein and is homozygous lethal. We reported that FSC clones that are homozygous for ben^{A} were more abundant than controls, suggesting that it causes FSC niche hypercompetition (Cook et al., 2017). However, this was not confirmed, and the cause of this phenotype and the specific roles of Ben in the early FSC lineage were not investigated.

In this study, we identify multiple, genetically distinct roles for Ben in the early FSC lineage. First, we demonstrate that Ben and other core components of the JNK pathway are required for specification of the stalk cell fate. Second, we show that

Department of Anatomy and Department of OB/Gyn-RS, University of California, San Francisco, Center for Reproductive Sciences, Eli and Edythe Broad Center of Regenerative Medicine and Stem Cell Research, 513 Parnassus Avenue, San Francisco, CA, 94143, USA.

*Author for correspondence (todd.nystul@ucsf.edu)

S.T., 0000-0002-7604-1138; J.P., 0000-0002-9442-1257; T.N., 0000-0002-6250-2394

Handling Editor: Cassandra Extavour
Received 23 March 2021; Accepted 13 October 2021

Development (2021) 148, dev199630. doi:10.1242/dev.199630

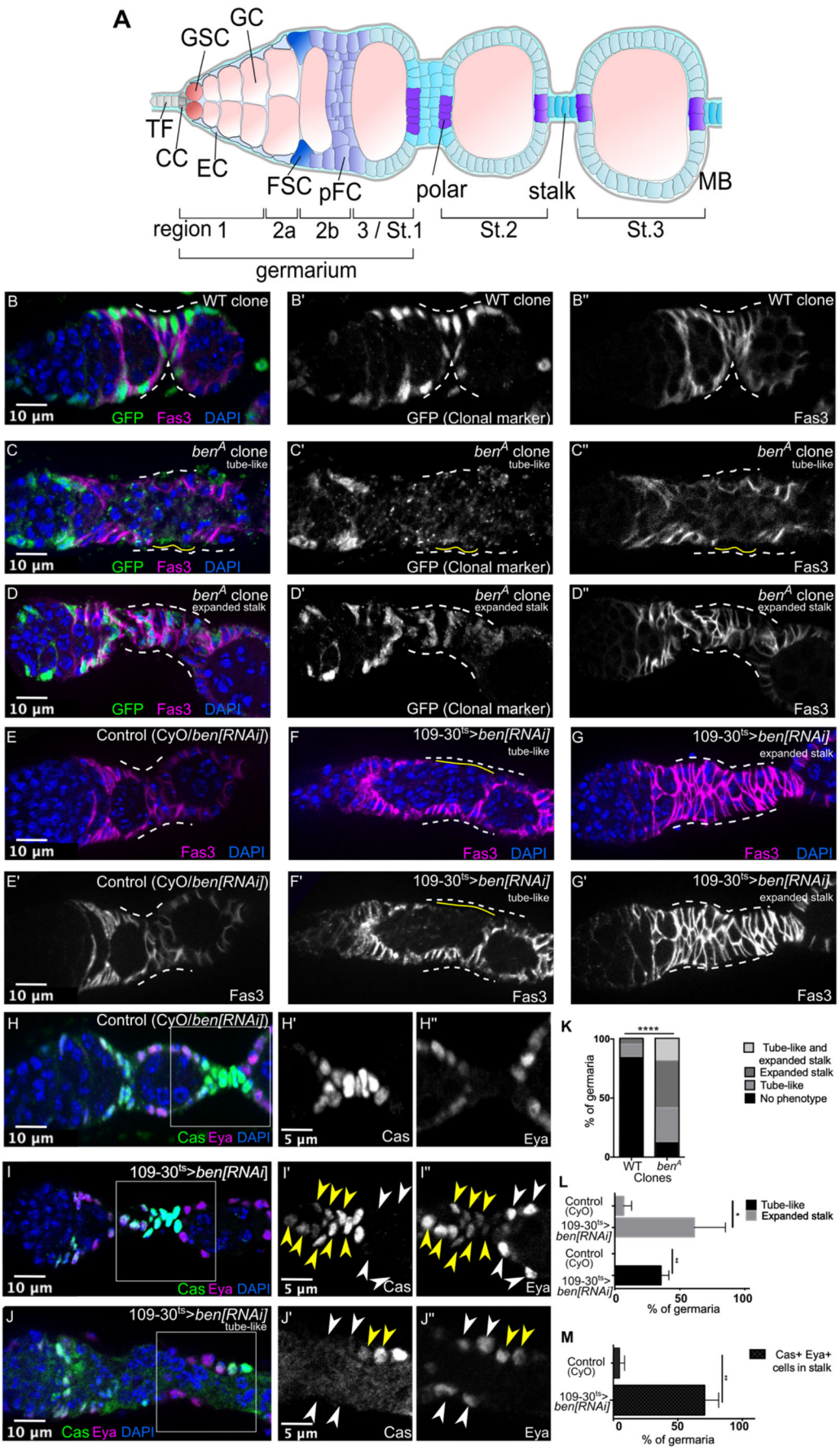

Fig. 1. See next page for legend.

Development (2021) 148, dev199630. doi:10.1242/dev.199630

Fig. 1. Ben is required for stalk cell specification and follicle formation. (A) Schematic of the germarium depicting terminal filament cells (TF), cap cells (CC), germline stem cells (GSC), germ cells (GC), in region follicle stem cells (FSC), pre-follicle cells (pFC), polar, stalk and main body follicle cells (MB). EC, escort cells. The germarium is divided into Region 1, Region 2a (2a), Region 2b (2b) and Region 3 (3), which is also called Stage 1 (St. 1). The first and second fully budded follicles are referred to as Stage 2 (St. 2) and Stage 3 (St. 3), respectively. (B-D″) Ovarioles with wild-type (WT) or ben^{A} GFP^{-} clones stained for Fas3 (magenta), GFP (green), and DAPI (blue). In wild-type ovarioles, stalk cells form into a single row of cells between adjacent follicles. In ovarioles with ben^{A} clones we observed gaps in the follicle epithelium (yellow lines), and the stalk regions can be absent, causing adjacent follicles to merge together ('tube-like phenotype', C) or cells can accumulate in this region and fail to intercalate into a single row ('expanded stalk phenotype', D). In all cases, the clones extend well beyond the germarium, and the ovarioles are mosaic or fully marked by the lack of GFP. (E-G′) Ovarioles with *ben[RNAi]* over a CyO balancer (Control) (E) or with *109-30^{ts}* driving expression of *ben[RNAi]* (F,G) stained with Fas3 (magenta) and DAPI (blue). The stalk regions in panels B-G are indicated with white dashed lines. (H-J″) Ovarioles with *ben[RNAi]* alone (H) or with *109-30^{ts}* driving expression of *ben[RNAi]* (I,J) stained for Eya (magenta), Cas (green) and DAPI (blue). In control germaria, stalk cells are Cas^{+}, Eya^{-} and main body cells are Cas^{-}, Eya^{+} (H). With knockdown of *ben*, the main body cells are still Cas^{-}, Eya^{+} (white arrowheads), but there are Cas^{+}, Eya^{+} cells in the stalk region (yellow arrowheads) (I,J). (K) Quantification of the frequency of germaria with tube-like and expanded stalk phenotype in ovarioles with mosaic or fully marked WT and ben^{A} mutant clones. Chi-squared test: ****P<0.0001, n≥68 ovarioles. (L) Quantification of the frequency of germaria with tube-like and expanded stalk phenotype in germaria with *ben[RNAi]* alone or *109-30^{ts}* driving expression of *ben[RNAi]*. Unpaired, two-tailed Student's *t*-test: **P<0.01, *P<0.05, N=3 flies, n≥84 ovarioles. (M) Quantification of the frequency of germaria with Cas^{+}, Eya^{+} in the stalk region in germaria with *ben[RNAi]* alone or *109-30^{ts}* driving expression of *ben[RNAi]*. Unpaired, two-tailed Student's *t*-test: **P<0.01, N=3 flies, n≥79 ovarioles. Data are mean±s.d.

Ben regulates the level of Hh signaling and the rate of proliferation in pFCs, whereas the downstream JNK pathway component, Hemipterous (Hep) does not. We also provide evidence that Ben, but not JNK signaling, may contribute to the specification of the main body cell fate at this stage. In addition, we test the association between hypercompetition, increased proliferation and Hh signaling in ben^{A} mutants, and find that overexpression of the cell cycle inhibitor Dacapo (Dap) or reduction of the Hh pathway effector Smoothened (Smo) is sufficient to suppress the hypercompetition phenotype. However, we show that *hep* mutant clones are not hypercompetitive, indicating that hypercompetition of ben^{A} mutant clones is a JNK-independent effect. Taken together, these findings demonstrate that Ben has distinct roles in the regulation of proliferation and differentiation in the FSC lineage and that a layer of regulation exists that acts to both downregulate niche signals in newly-produced pFCs and promote the activation of differentiation cues.

RESULTS

Ben is required for follicle formation and stalk cell specification

To investigate the function of Ben in the early FSC lineage, we first determined the expression pattern of *ben* in the ovary. We found that *ben* RNA is detectable in all cell types that were profiled in our recent ovarian cell atlas (Fig. S1A) (Rust et al., 2020). To confirm this *in vivo*, we assayed for *ben* transcripts in the germarium using fluorescence *in situ* hybridization chain reaction (HCR) (Choi et al., 2018) and, indeed, we observed that *ben* is broadly expressed, including in FSCs and pFCs. This signal was substantially reduced in follicle cells with the expression of *ben[RNAi]* using the early follicle cell Gal4 driver *109-30-Gal4* (Hartman et al., 2010), which indicates that the signal is specific for *ben* transcripts and confirms that the RNAi line is effective (Fig. S1B,C).

Next, we stained ovarioles with wild-type or ben^{A} clones that are marked by the lack of GFP (GFP^{-}) for Fas3, which marks membranes of early follicle cells, and examined the tissue morphology. We found that ovarioles in which the follicle cell population in the germarium was mosaic (partially marked) or only consisted of ben^{A} mutant cells (fully marked) had a range of follicle formation defects, including gaps in the follicle epithelium, 'tube-like' phenotypes characterized by defective or absent stalks between the germarium and the downstream follicles, and 'expanded stalk' phenotypes characterized by the presence of extra cells in the stalk region that form multiple rows (Fig. 1B-D,K; Fig. S2A-D) (Berns et al., 2014). We also noticed a small but significant increase in the frequency of ovarioles with follicle formation defects in ben^{A}/+ heterozygous flies compared with wild-type controls (Fig. S2E), but the frequencies of follicle formation phenotypes were not significantly different between ben^{A}/+ ovarioles with or without ben^{A} homozygous germ cell clones (Fig. S2E). This suggests that *ben* is not required in germ cells for follicle formation. We observed similar phenotypes in ovarioles with *ben[RNAi]* driven in early follicle cells specifically during adulthood using *109-30-Gal4* and *tub-Gal80^{ts}* (McGuire et al., 2003) (referred to hereafter as *109-30^{ts}*), though the expanded stalk phenotype was more common in this context (Fig. 1E-G,L). This confirms that reduction of *ben* expression in the early FSC lineage causes follicle formation defects.

As stalk cell specification is initiated in a subset of pFCs in the early FSC lineage, tube-like and expanded stalk phenotypes suggest a defect in pFC differentiation (Berns et al., 2014). To further assay for follicle cell differentiation defects upon knockdown of *ben*, we stained ovarioles with *ben[RNAi]* driven by *109-30^{ts}* for Castor (Cas) and Eyes absent (Eya). In control ovarioles, early pFCs express high levels of both Cas and Eya and then become either Cas^{+}, Eya^{-} as they differentiate into stalk or polar cells, or Cas^{-}, Eya^{+} as they differentiate into main body follicle cells (Fig. 1H) (Bai and Montell, 2002; Chang et al., 2013). We found that a majority (70.9%±10.9%, n=30) of ovarioles with *ben[RNAi]* driven by *109-30^{ts}* contained Cas^{+}, Eya^{+} cells in the regions between follicles, where stalk cells typically reside (Fig. 1I-J,M). However, the main body follicle cells surrounding recently budded follicles in these mutant ovarioles were Cas^{-}, Eya^{+} (Fig. 1I-J) indicating that, unlike the cells in the stalk region, they were able to exit the Cas^{+}, Eya^{+} state associated with pFC identity. Taken together, these results suggest that the follicle formation defects caused by knockdown of *ben* are due, at least in part, to a failure of mutant pFCs to differentiate into stalk cells.

JNK signaling is required for pFC differentiation

Ben is a positive regulator of JNK signaling in the *Drosophila* eye and wing discs (Herrera and Bach, 2021; Ma et al., 2014), so we hypothesized that the follicle formation defects in *ben* mutants are due to impaired JNK signaling. JNK signaling is activated when a secreted ligand, Eiger (Egr), binds to a cell surface receptor, Grindelwald (Grnd) or Wengen (Wgn), to initiate a cascade of intracellular events (Fig. S3A). First, Ben and the E3 ubiquitin ligase, TNF-receptor-associated factor 6 (Traf6), ubiquitylate the upstream kinase, TGF-β activated kinase 1 (TAK1), which then phosphorylates and activates downstream kinases, Basket (Bsk) and Hep, ultimately leading to the activation of the transcription factor complex, AP-1 (Tafesh-Edwards and Eleftherianos, 2020). We found that *hep* RNA is expressed broadly throughout the germarium

Development (2021) 148, dev199630. doi:10.1242/dev.199630

and early follicles (Fig. S1A,D-E) and that the synthetic JNK signaling reporter AP-1-GFP (Chatterjee and Bohmann, 2012; Harris et al., 2016) is detectable in escort cells and stalk cells (Fig. 2A). In ovarioles with *ben*^{A} follicle cell clones, AP-1-GFP expression was absent in stalk cells, indicating that Ben positively regulates JNK signaling in the FSC lineage (Fig. 2B).

To determine whether other components of the JNK pathway are required for follicle formation and early pFC differentiation, we depleted expression of Hep, Egr, Grnd or Bsk using RNAi in early follicle cells during adulthood and stained for Fas3. Indeed, knockdown of any of these genes caused both tube-like and expanded stalk phenotypes (Fig. 2C-F; Fig. S3B-G). To further confirm the requirement of Hep for stalk differentiation, we generated follicle cell clones that are homozygous for *hep*^{G0107}, which is a recessive lethal mutation (Baril et al., 2009; Guichard et al., 2006). Again, we observed ovarioles with tube-like and expanded stalk phenotypes (50.9%; Fig. 2G,H,K). Moreover, as with knockdown of *ben*, we observed cells within the expanded stalks of *hep[RNAi]* mutants that were still Cas^{+}, Eya^{+}, whereas the cells in the main body cell region had matured into the Cas^{-}, Eya^{+} state (Fig. 2I,J,L). This suggests that RNAi knockdown of Hep impairs differentiation of pFCs into stalk cells. Collectively, these experiments confirm that Ben positively regulates JNK signaling in follicle cells, and that JNK signaling is necessary for pFC differentiation into stalk cells.

Loss of JNK signaling impairs the activation of the Notch signaling reporter *NRE-GFP*

Stalk cells are specified by JAK-STAT signaling from polar cells, and differentiation toward the polar cell fate is induced in early pFCs by Notch signaling (Assa-Kunik et al., 2007; Dai et al., 2017; Lopez-Schier and St Johnston, 2001). Therefore, we next investigated whether a loss of JNK signaling impairs JAK-STAT or Notch signaling in the FSC lineage. Consistent with previous results (Melamed and Kalderon, 2020; Vied et al., 2012), we found that the JAK-STAT reporter *10x-STAT-GFP* (Bach et al., 2007) is

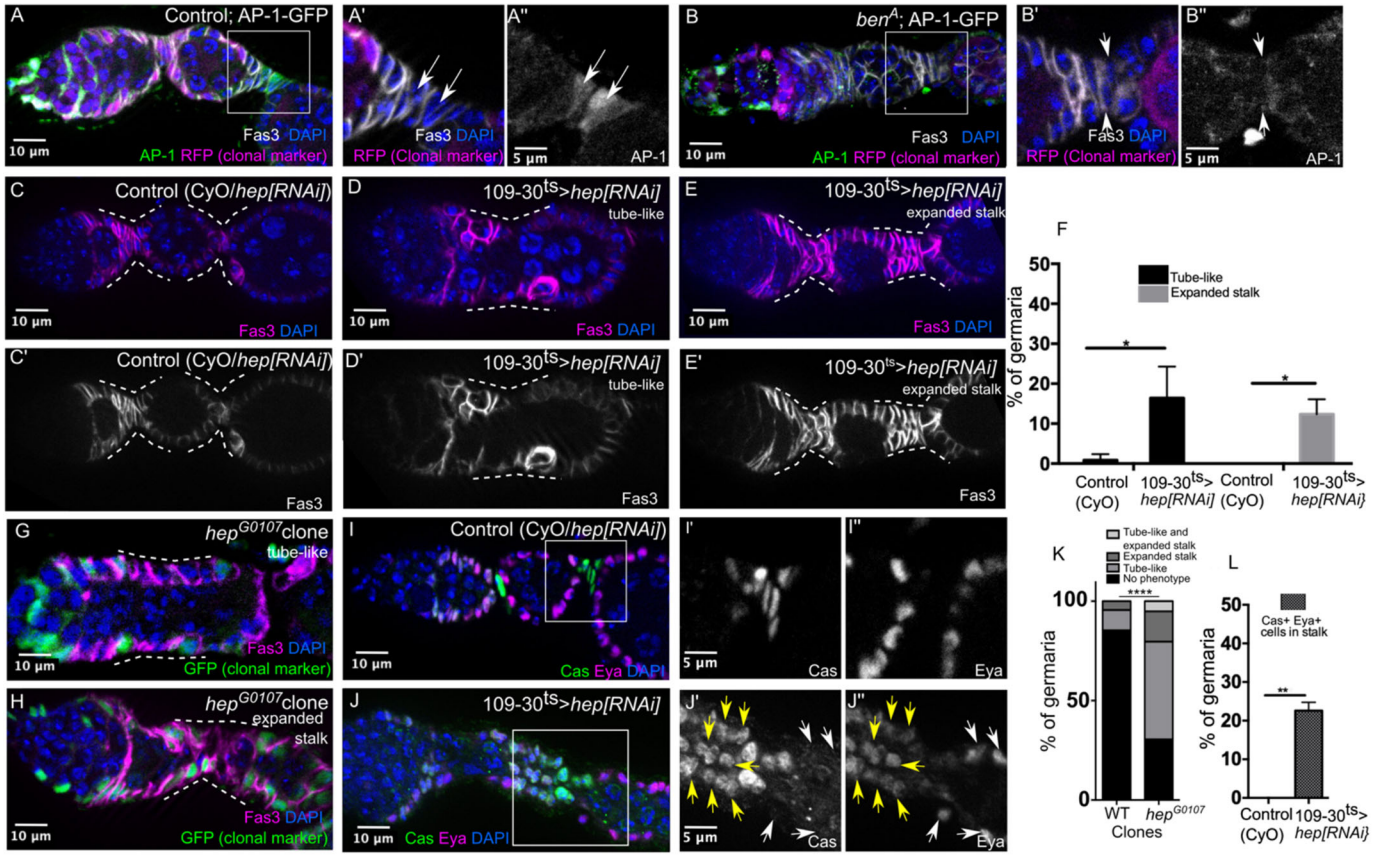

Fig. 2. JNK signaling is required for pFC differentiation and follicle formation. (A-B″) Ovarioles with the *AP-1-GFP* reporter and wild-type control (A) or *ben*^{A} RFP^{-} clones (B) stained for Fas3 (white), RFP (magenta), GFP (green) and DAPI (blue). AP-1-GFP reporter activity is present in wild-type stalk cells but absent in *ben*^{A} stalk cells (white arrows). (C-E′) Ovarioles with *hep[RNAi]* alone (C) or *109-30*^{ts} driving expression of *hep[RNAi]* (D-E′) stained with Fas3 (magenta) and DAPI (blue). Wild-type stalk morphology is present in control ovarioles (white dashed line, C); tube-like stalk phenotype (white dashed line, D) and expanded stalk phenotype (white dashed line, E) are present in ovarioles with *109-30*^{ts} driving expression of *hep[RNAi]*. (F) Quantification of the frequency of germaria with tube-like and expanded stalk phenotype in germaria with *hep[RNAi]* alone or *109-30*^{ts} driving expression of *hep[RNAi]*. Student's *t*-test: *P<0.05, N=3 flies, n≥84 ovarioles. (G,H) Ovarioles with *hep*^{G0107} mutant clones stained for Fas3 (magenta), GFP (green) and DAPI (blue). Clones are marked by the lack of GFP. Tube-like phenotype (G) or expanded stalk phenotype (H) present in ovarioles with *hep*^{G0107} mutant clones. (I-J″) Ovarioles with *hep[RNAi]* alone (I) or *109-30*^{ts} driving expression of *hep[RNAi]* (J) stained with Eya (magenta), Cas (green) and DAPI (blue). Control germaria contain Cas^{+}, Eya^{-} cells in stalk region and Cas^{-}, Eya^{+} cells in main body cell region (I), but Cas^{+}, Eya^{+} cells in the stalk region (yellow arrows) and Cas^{-}, Eya^{+} cells in the main body cell region (white arrowheads) in germaria expressing *hep[RNAi]* (J). (K) Quantification of frequency of germaria with tube-like and expanded stalk phenotype in ovarioles with mosaic or fully marked wild-type (WT) and *hep*^{G0107} mutant clones. Chi-squared test: ****P<0.0001, n≥59. (L) Quantification of the frequency of germaria with Cas^{+}, Eya^{+} in the stalk region in germaria with *hep[RNAi]* alone or *109-30*^{ts} driving expression of *hep[RNAi]*. Unpaired, two-tailed Student's *t*-test: **P<0.01, N=3 flies, n≥86 ovarioles. Data are mean±s.d.

Development (2021) 148, dev199630. doi:10.1242/dev.199630

active throughout the early FSC lineage in wild-type ovarioles. This pattern was unaffected in ben^{A} or hep^{G0107} clones, indicating that JNK signaling is not required for JAK-STAT signaling in the FSC lineage (Fig. S4). The Notch pathway reporter, *NRE-GFP*, was detectable in wild-type ovarioles at the Region 2a/2b border where Notch signaling induces differentiation toward the polar cell fate, and again in mature polar cells starting in Region 3/Stage 1 follicles, as expected (Dai et al., 2017; Johnston et al., 2016). In contrast, the *NRE-GFP* signal was absent from the Region 2a/2b border and in mature polar cells in some germaria with ben^{A} or hep^{G0107} clones, suggesting that loss of JNK signaling impairs Notch pathway activation in follicle cells (Fig. 3A-C). The cells in this region are closely packed together and only a subset normally expresses *NRE-GFP*. Thus, to simplify the comparison between genotypes, we focused on germaria in which all follicle cells in the germarium were marked by the lack of GFP, and thus part of a clone. In wild-type controls, 83.3% (n=12) of germaria had detectable *NRE-GFP* signal in Region 2b, whereas this frequency was significantly lower in germaria with ben^{A} (36.4%, n=22) or hep^{G0107} (0%, n=12) mutant clones (Fig. 3A-C,G). In addition, we found that the *NRE-GFP* signal was also frequently absent from mature polar cells, which can be identified as small clusters of cells with high levels of Fas3 staining, in ben^{A} or hep^{G0107} mutant clones compared with controls (Fig. 3D-F,H). However, as Notch signaling in Region 2b is required for the differentiation of pFCs into polar cells, and we frequently observed polar cell clusters in ben^{A} and hep^{G0107} clones (Fig. 3D-F), the functional significance of the loss of *NRE-GFP* signal in pFCs is unclear.

Impaired JNK signaling causes retention of phosphorylated ERK in pFCs, which blocks pFC differentiation

The transition from the FSC to pFC fate is characterized by an abrupt decrease in the level of double phosphorylated ERK (pERK), which is an indicator of EGFR signaling, and a gradual decrease in *Ptc-pelican-GFP*, which is a reporter of Hh signaling (Castanieto et al., 2014; Sahai-Hernandez and Nystul, 2013). To determine whether *ben* mutants affect the pattern of pERK, we first generated ovarioles with ben^{A} mutant clones or *ben[RNAi]* driven with either $109\text{-}30^{ts}$ or the pFC driver *stl-Gal4*, and stained for pERK. We found that pERK was clearly detectable in cells at the Region 2a/2b border, and then downregulated in Region 2b in the control ovarioles, as reported previously (Castanieto et al., 2014). In contrast, the pERK signal was strong in pFCs throughout Region 2b in ovarioles with either ben^{A} clones or with *ben[RNAi]* driven by $109\text{-}30^{ts}$ or $stl\text{-}Gal4^{ts}$ (Fig. 4A-E,J; Fig. S5A,B). We even observed a small but significant increase in the frequency of ovarioles with $pERK^{+}$ pFCs in ben^{A}/+ ovarioles (Fig. 4C, 'unmarked' category). Likewise, RNAi knockdown of the JNK pathway components *egr*, *grnd*, *traf6* or *hep* driven by $109\text{-}30^{ts}$ or *hep* driven by $stl\text{-}Gal4^{ts}$ also caused retention of pERK in pFCs throughout Region 2b (Fig. 4D, F-J; Fig. S5C). To determine whether other aspects of EGFR signaling are affected, we assayed for cell polarity defects in ben^{A} mutants. Constitutive activation of EGFR signaling interferes with the maturation of apical cell polarity in the early FSC lineage (Castanieto et al., 2014). However, we observed no defects in the localization of apical or lateral markers in ben^{A} pFCs (Fig. S6), indicating that, although loss of JNK signaling causes retention of pERK in pFCs, it does not phenocopy the impaired maturation of cell polarity that has been observed with constitutive EGFR signaling (Castanieto et al., 2014).

To explore whether activation of ERK affects pFC differentiation, we overexpressed a constitutively active allele, ERK^{SEM}, in the early FSC lineage during adulthood with $109\text{-}30^{ts}$ and stained for Fas3, Cas and Eya. Indeed, upon overexpression of ERK^{SEM}, we observed a significant increase in ovarioles with an expanded stalk, a tube-like phenotype, or both, compared with controls (Fig. 5A-C,F; 56.3%, $n \geq 114$). In addition, we found Cas^{+}, Eya^{+} cells within the stalk region in a majority of mutant ovarioles (Fig. 5D,E,G; 75.8%±25.0%, $n \geq 88$). As with knockdown of JNK pathway components, the cells in the main body cell region were Cas^{-}, Eya^{+}. These observations indicate that increased ERK activity in pFCs impairs differentiation toward the stalk cell fate and suggest that the aberrant activation of ERK contributes to the pFC differentiation defects we observed in ovarioles with impaired JNK signaling in the early follicle cell lineage.

Ben functions in a JNK pathway-independent manner to promote Hh signaling in FCs

Next, we assayed for *Ptc-pelican-GFP* expression in wild-type and mutant tissue. In wild-type ovarioles, we observed a progressive decrease of *Ptc-pelican-GFP* expression throughout Region 2b (Fig. 6A), as expected (Sahai-Hernandez and Nystul, 2013; Ulmschneider et al., 2016). In contrast, the *Ptc-pelican-GFP* signal was significantly higher in ben^{A} cells throughout Region 2b, and remained clearly detectable in follicle cells throughout the germarium (Fig. 6B,D,E). However, we did not observe a significant increase in *Ptc-pelican-GFP* signal in hep^{G0107} cells throughout Region 2b (Fig. 6C,F). To further explore the effect of Hh signaling, we assayed for *zfh1* expression, which is known to be expressed in ovarian somatic cells and is a direct target of Hh signaling in the *Drosophila* testis (Michel et al., 2012). In wild-type germaria, *zfh1* is consistently expressed in escort cells, FSCs, pFCs in Region 2b and stalk cells, and tapers off in the pFCs in Region 3 (Fig. 6G). Specifically, only 62.9%±16.8 of germaria have $Zfh1^{+}$ pFCs in Region 3, and *zfh1* expression is completely absent in the main body follicle cells of the first budded follicle downstream from the germarium (referred to as a Stage 2 follicle). Overexpression of *Hh* driven with $109\text{-}30^{ts}$ induced the expression of *zfh1* in follicle cells throughout Region 3 and Stage 2 follicles, indicating that, as in the testis, *zfh1* expression is activated by Hh signaling in the follicle epithelium (Fig. 6H). In ovarioles with RNAi knockdown of *ben*, we observed a significant increase in the number of germaria with $Zfh1^{+}$ follicle cells in Region 3 and Stage 2 follicles (Fig. 6I,K). In contrast, RNAi knockdown of *hep* driven by $109\text{-}30^{ts}$ had no effect on the pattern of *Ptc-pelican-GFP* or *zfh1* expression (Fig. 6J,L). These observations indicate that Ben functions in a JNK pathway-independent manner to shape the patterning of Hh signaling in pFCs and main body follicle cells of newly budded follicles.

Loss of Ben increases proliferation in pFCs

Hedgehog signaling regulates proliferation in the early FSC lineage (Hartman et al., 2010, 2013; Huang and Kalderon, 2014; Singh et al., 2018; Zhang and Kalderon, 2000), so our finding that *ben* mutants have increased Hh signaling raised the possibility that the rate of proliferation may also be increased. To test this possibility, we used EdU assays, which identify cells in S-phase, in ovaries with wild-type, hep^{G0107} or ben^{A} GFP^{-} clones. In wild-type mosaic ovarioles, we found no significant difference in the percentages of EdU^{+} cells (i.e. the 'proliferation indices') in the GFP^{-} and GFP^{+} populations, as expected. Consistent with our finding that hep^{G0107} mutant pFCs do not have increased levels of Hh signaling, we observed no significant difference in the proliferation indices of hep^{G0107} homozygous mutant follicle cells compared with hep^{G0107}/+ heterozygous cells. By contrast, in mosaic ovarioles

Development (2021) 148, dev199630. doi:10.1242/dev.199630

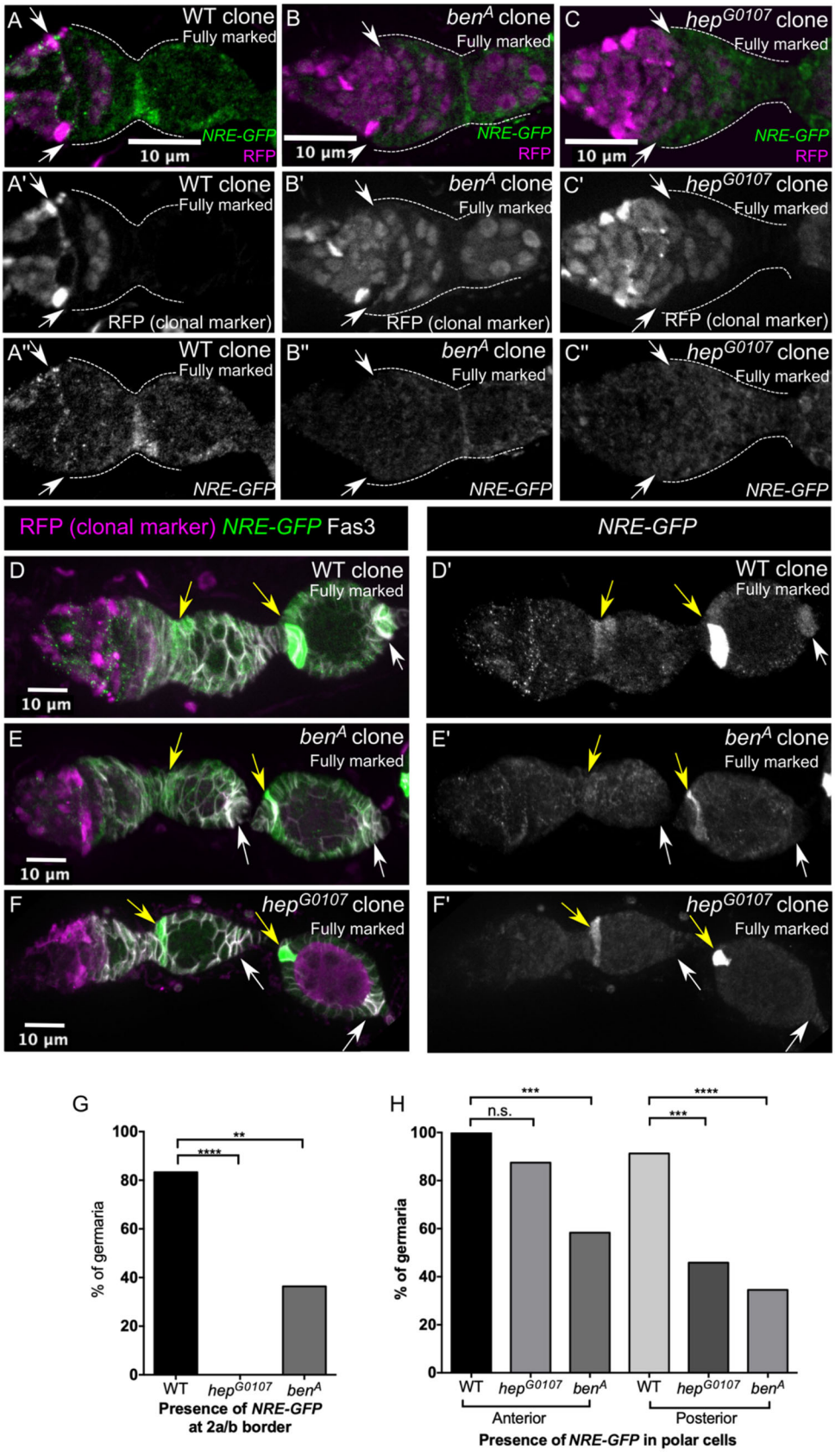

Fig. 3. JNK signaling is required for the normal expression of the Notch signaling reporter *NRE-GFP*. (A-F′) Ovarioles in which the follicle cell populations in the germarium and first two follicles are fully marked by the lack of RFP stained for GFP (green), RFP clonal label (magenta) and Fas3 (white). The RFP$^-$ clones are either a wild-type control (WT) (A,D), *ben*^{A} (B,E) or *hep*^{G0107} (C,F). The germarium is outlined with white dashed lines in A-C, the Region 2a/2b border is indicated with white arrows in A-C, the anterior polar cell clusters are indicated with yellow arrows in D-F and the posterior polar cell clusters are indicated with white arrows in D-F. (G,H) Quantifications of the frequencies of germaria with *NRE-GFP* expression at the 2a/b border (G) and *NRE-GFP* expression in anterior and posterior polar cell clusters (H) in germaria with WT, *hep*^{G0107} and *ben*^{A} mutant clones. The *NRE-GFP* signal is typically detectable in all three of these locations in the control ovarioles but is detectable in these locations at lower frequencies in *ben*^{A} or *hep*^{G0107} mutant ovarioles. Chi-squared test: ****P<0.0001, ***P<0.001, **P<0.01, $n\geq12$ ovarioles. n.s., not significant.

with *ben*^{A} clones, we observed a significantly higher proliferation index in the GFP$^-$ (*ben*^{A}/*ben*^{A}) population compared with the GFP$^+$ (*ben*^{A}/+) population (Fig. 7A-D). Likewise, we observed a significant increase in the EdU proliferation index in ovarioles that are fully marked *ben*^{A} follicle cell clones compared with ovarioles that are fully marked with wild-type control clones

Development (2021) 148, dev199630. doi:10.1242/dev.199630

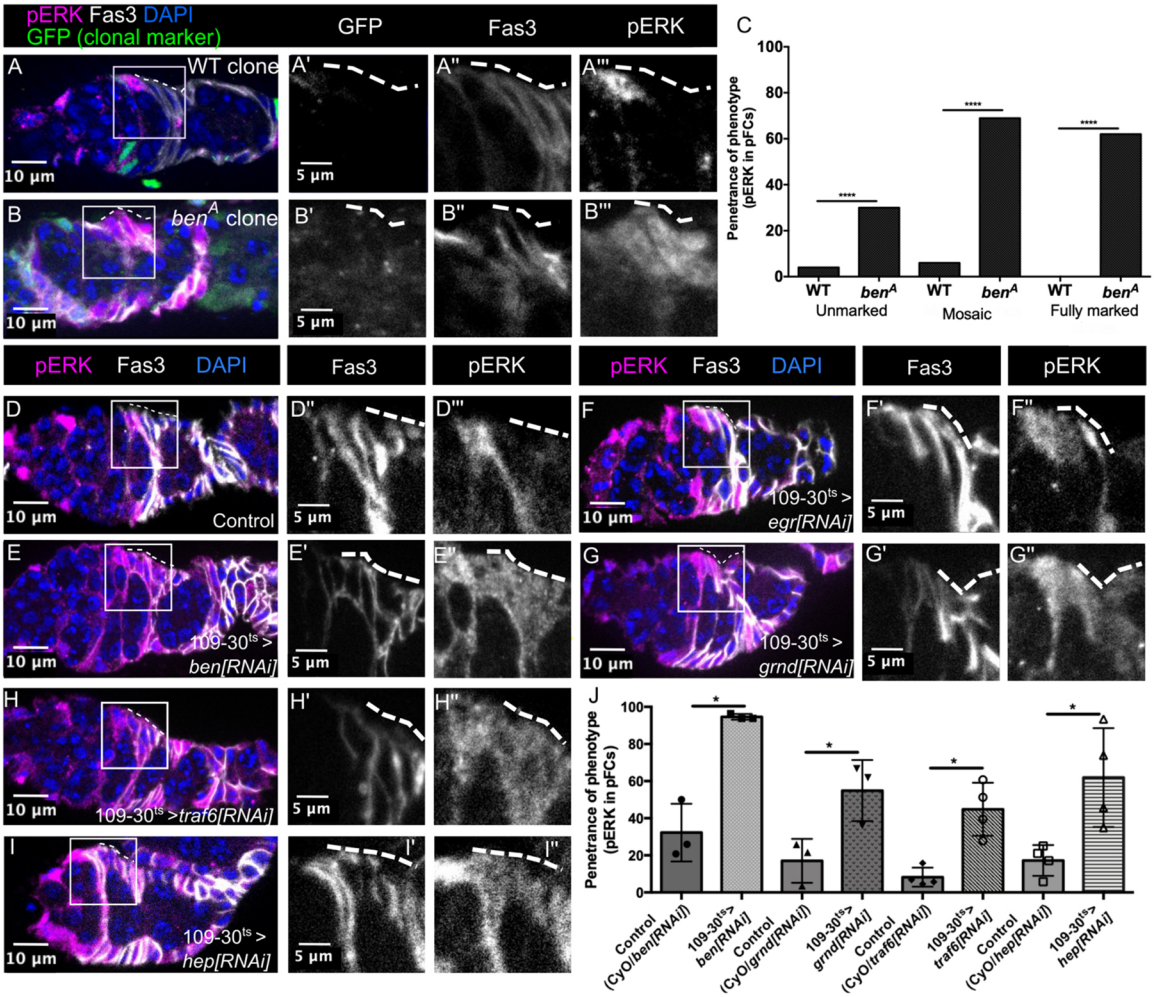

Fig. 4. JNK signaling is required to decrease pERK in pFCs. (A-B‴) Ovarioles with wild-type (WT) or *ben*^{A} GFP^{-} clones stained for GFP (green), pERK (magenta), Fas3 (white) and DAPI (blue). The pERK signal is absent in the pFCs within control clones (white dashed lines, A), but clearly detectable in pFCs within *ben*^{A} clones (white dashed lines, B). (C) Quantification of the frequency of ovarioles with pERK signal in pFCs in ovarioles that have all GFP^{+} (unmarked) follicle cells, a mosaic population of follicle cells, or all GFP^{-} follicle cells (fully marked). Chi-squared test: ****P<0.0001, n≥20 unmarked clones, n≥42 mosaic and n≥20 fully marked follicle cell lineage. (D-I″) Ovarioles with *109-30*^{ts} alone (D) or *109-30*^{ts} driving expression of RNAi against *ben*, *egr*, *grnd*, *traf6* or *hep* (E-I, respectively) stained for Fas3 (white), pERK (magenta) and DAPI (blue). The pERK signal is absent in pFCs in the control ovarioles (white dashed lines, D) but clearly detectable in the pFCs of the mutant ovarioles (white dashed lines, E-I). (J) Quantification of the frequency of germaria with the pERK signal in pFCs in the indicated genotypes and their paired controls (*109-30*^{ts} alone). Unpaired, two-tailed Student's *t*-test: *P<0.05, N≥3 flies, n≥79 ovarioles. Data are mean±s.d.

(Fig. 7E-G). Consistent with these results, we also observed a significantly higher frequency of cells that are positive for the M-phase marker phosphohistone H3 (pH3) in fully marked ovarioles with *ben*^{A} clones compared with those with wild-type clones (Fig. 7H-K).

To confirm that the increased proliferation is due to a reduction of Ben but not Hep function, we also compared the proliferation indices of the follicle cell populations in germaria with *ben[RNAi]* or *hep[RNAi]* driven by *109-30*^{ts} with wild type. Again, compared with the wild-type control, we observed a significant increase in proliferation indices in germaria with *ben[RNAi]*, but not *hep[RNAi]* (Fig. 7L). Taken together, these observations suggest that Ben has at least two distinct functions in the regulation of pFC differentiation: a JNK pathway-dependent role in the regulation of pFC differentiation through the downregulation of pERK and possibly also increased receptivity to Notch signaling, and a JNK pathway-independent role in the regulation of Hh signaling and proliferation within the early FSC lineage.

Loss of Ben causes hypercompetition in the FSC niche by regulating pFC proliferation and differentiation

Previous studies have shown that FSCs can be lost and replaced by cells from a neighboring FSC lineage (Kronen et al., 2014; Nystul and Spradling, 2007; Wang et al., 2012). In these studies, FSC clones are generated with a lineage tracing system that marks the FSCs and their progeny with a genetically heritable label, such as the lack of GFP (in a negatively-marked system; Fig. 8A) or the expression of GFP (in a positively-marked system) (Fox et al., 2008; Hafezi and Nystul, 2001). When the lineage tracing system is used to label FSCs in an otherwise wild-type tissue, the marked and unmarked cells are functionally equivalent, and the pattern of FSC loss and replacement conforms to a model of neutral competition for niche occupancy (Clayton et al., 2007; Klein and Simons, 2011; Kronen et al., 2014). If the lineage tracing system simultaneously marks the cells and introduces a genetic mutation, the effect of the mutation on FSC niche competition can be tested by quantifying the changes in the frequencies of ovarioles with either an unmarked

Development (2021) 148, dev199630. doi:10.1242/dev.199630

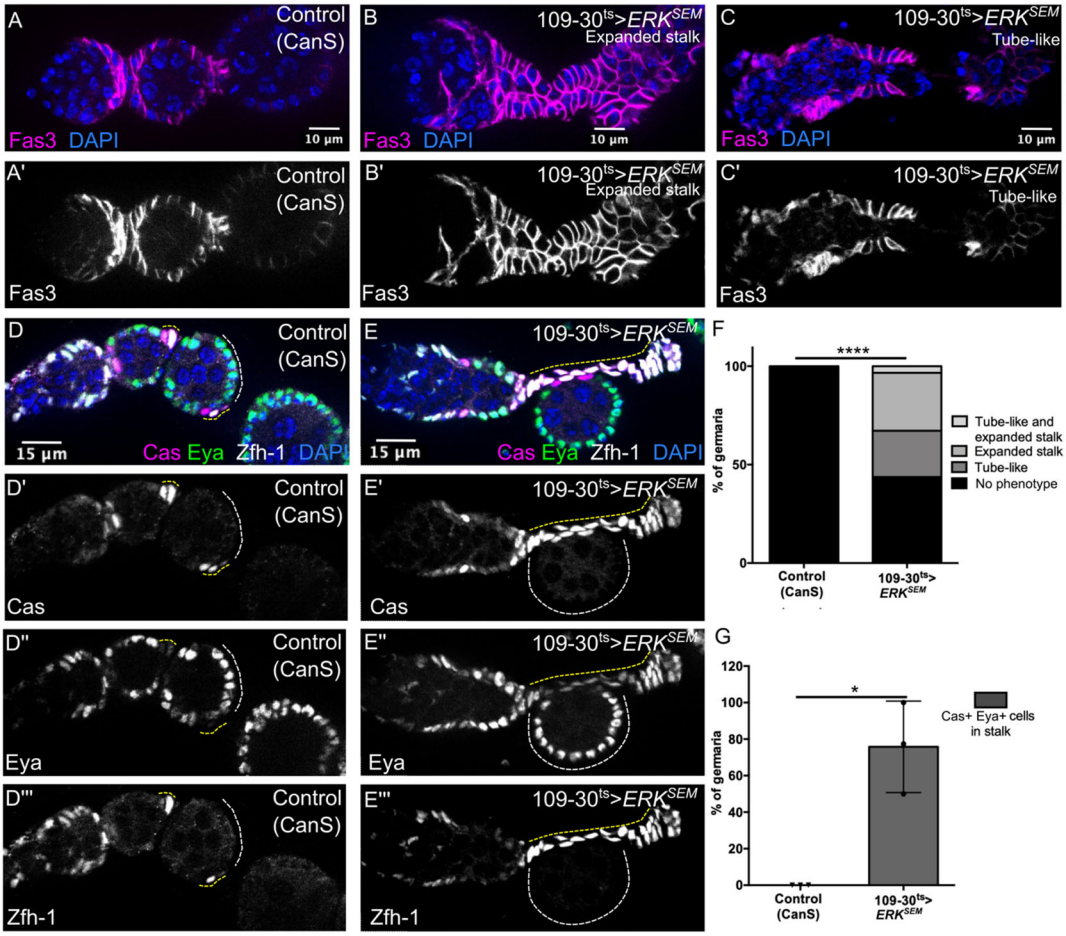

Fig. 5. Constitutively active *ERK* in the FC lineage causes defects in stalk formation and differentiation. (A-E‴) Ovarioles from the Canton-S (CanS) wild-type strain (A) or with *109-30^{ts}* driving expression of *ERK^{SEM}*, a constitutively active allele of *ERK*, (B,C) stained for Fas3 (magenta) and DAPI (blue) in panels A-C or Cas (magenta), Eya (green), Zfh1 (white) and DAPI (blue) in panels D,E. Overexpression of *ERK^{SEM}* causes expanded stalk phenotypes (B), tube-like phenotypes (C), and Cas^{+}, Eya^{+} cells in the stalk region (yellow dotted lines in E) but does not prevent the formation of Cas^{-}, Eya^{+} cells in the main body cell region (white dotted lines in E). The expression pattern of *zfh1* remained unaffected (D‴,E‴). Progeny were maintained at 18°C until eclosion, and then shifted to 29°C for 18 days. (F-G) Quantifications of the frequency of germaria with an expanded stalk or tube-like phenotype (F) or with Cas^{+}, Eya^{+} cells in the stalk region (G). Chi-squared test: ****P<0.0001, n≥114 (F) and unpaired, two-tailed Student's t-test: *P<0.0001, N=3 flies, n≥88 ovarioles (G). Data are mean±s.d.

(i.e. unrecombined), mosaic or fully marked (i.e. recombined) population of follicle cells in the germarium over time.

To confirm the hypercompetition phenotype of *ben^{A}*, we heat shocked flies to induce wild-type control or *ben^{A}* mutant clones that are marked by the lack of GFP in adult flies, and quantified the proportion of germaria with fully GFP^{-}, mosaic or fully GFP^{+} follicle cell populations at 6, 12 and 18 days post heat shock (dphs) (Fig. 8B-D). We observed a significant increase in germaria with *ben^{A}* mutant clones compared with wild type, indicating that *ben^{A}* mutant cells are hypercompetitive for the FSC niche (Fig. 8E), consistent with our previous results (Cook et al., 2017). In addition, we found that FSCs mutant for *ben^{B}*, an allele of *ben* that contains a missense point mutation, also displayed FSC hypercompetition, tube-like morphological phenotypes and increased pERK in pFCs (Fig. 8E; Fig. S7). In contrast, the frequency of germaria with *hep^{G0107}* clones was not significantly different from the control, indicating that downregulation of JNK signaling does not affect FSC niche competition (Fig. 8E). To test whether the increased proliferation or increased Hh signaling that we observed in *ben^{A}* mutant clones is necessary for the hypercompetition phenotype, we used the GFP^{+} clonal marking system, MARCM (Lee and Luo, 2001) (Fig. 8F-I), to combine homozygosity for *ben^{A}* with expression of either *dap*, which slows the cell cycle by inhibiting cyclin-dependent kinases (Lane et al., 1996), or *smo[RNAi]*. Indeed, we observed a significant reduction in clones expressing *dap* or *smo[RNAi]* either alone or in combination with *ben^{A}* compared with the control (Fig. 8I). Overexpression of *dap* or RNAi knockdown of *smo* in *ben^{A}* clones completely reversed the hypercompetition phenotype of *ben^{A}* mutant clones, causing them to become hypocompetitive. Moreover, we confirmed that RNAi knockdown of *smo* significantly reduced the rate of proliferation in pFCs (Fig. 8J), as measured by EdU incorporation (Huang and Kalderon, 2014). Collectively, these results indicate that the hypercompetition phenotype of *ben^{A}* mutants is not due to the differentiation defects caused by abnormal JNK signaling and suggest instead that it is due to the increased rate of proliferation induced by elevated Hh signaling in these mutants.

DISCUSSION

The segregation of FSC and daughter cell fates requires the orchestration of multiple developmental signaling pathways to ensure that cell fate specification and proliferation occurs at the correct time and place. Here, we have identified a new layer of regulation in which a single gene, *ben*, has multiple distinct roles

Development (2021) 148, dev199630. doi:10.1242/dev.199630

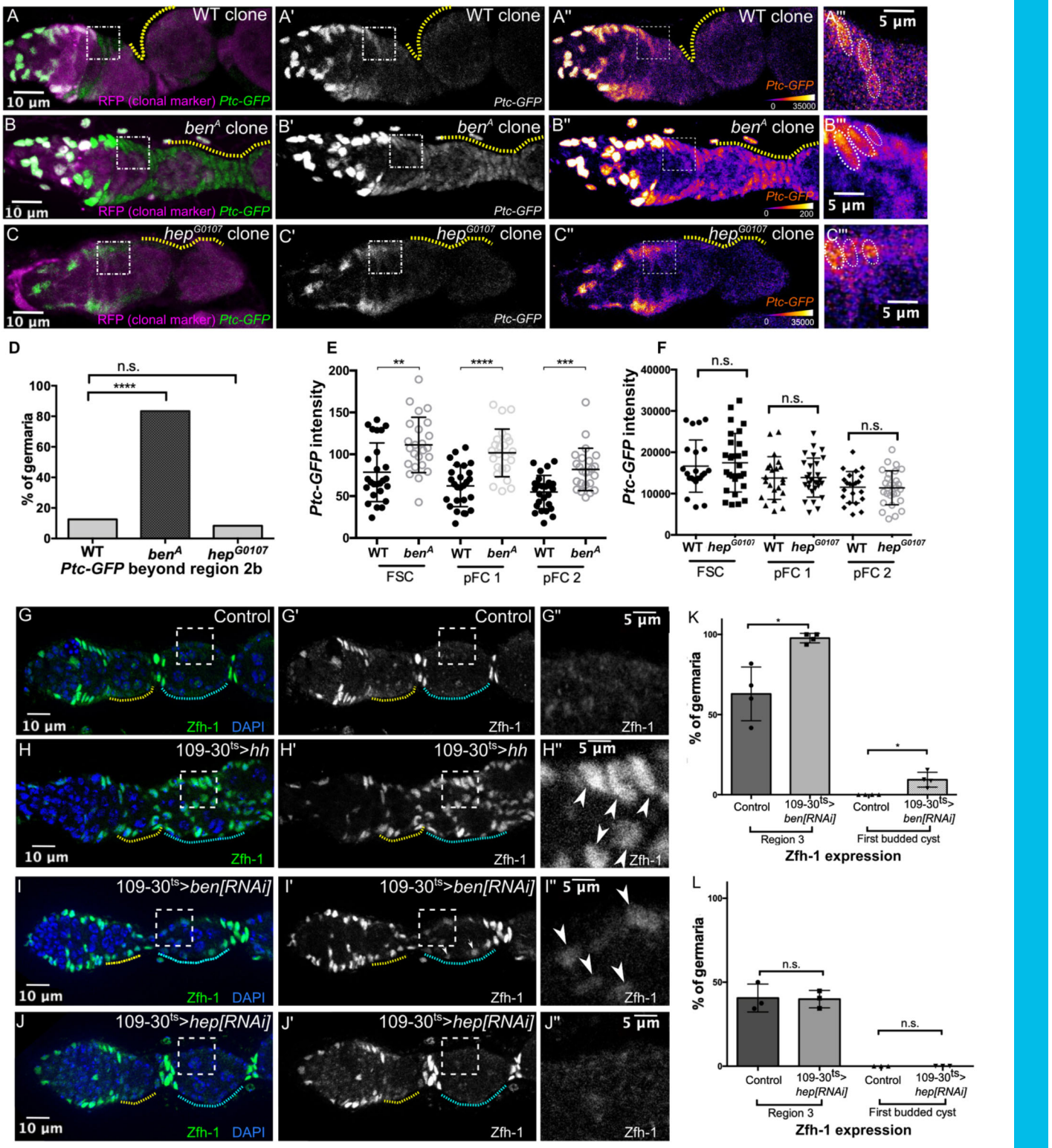

Fig. 6. Ben is required for proper patterning of Hh signaling in the early FSC lineage. (A-C‴) Ovarioles with *Ptc-pelican-GFP* and wild-type (WT), hep^{G0107} or ben^{A} RFP^{-} clones stained for RFP (magenta) and GFP (green). The *Ptc-pelican-GFP* channel is shown with colorimetric scale in A″-C″ to highlight differences in intensity. Measurements of the *Ptc-pelican-GFP* signal were taken from the FSC, identified as the anterior-most cell in the clone, and next two pFCs downstream from the FSC (white dotted lines in the boxed areas, magnified in A‴-C‴). (D-F) Quantifications showing percent of germaria with *Ptc-pelican-GFP* expressed beyond Region 2b (D), and *Ptc-pelican-GFP* intensity in FSCs and early pFCs (E,F) within clones of each genotype. Chi-squared test: $^{**}P<0.01$, $^{***}P<0.001$, $^{****}P<0.0001$, $n\geq12$ ovarioles. (G-J″) Ovarioles with *ben[RNAi]* or *hep[RNAi]* without *109-30^{ts}* (Control, G) or *109-30^{ts}* driving expression of *Hh* (H), *ben[RNAi]* (I) or *hep[RNAi]* (J), stained for Zfh1 (green) and DAPI (blue). Region 3 marked with yellow dotted lines and Stage 2 marked with cyan dotted lines. The boxed areas (magnified in G″-J″) show the aberrant expression of *zfh1* in main body cells of Stage 2 follicles upon overexpression of *Hh* or RNAi knockdown of *ben*, but not RNAi knockdown of *hep*. (K,L) Quantifications of the frequency of ovarioles in which *zfh1* is expressed in follicle cells in Region 3 and Stage 2 follicles in the indicated genotypes. Unpaired, two-tailed Student's *t*-test, $^{*}P<0.05$, $N\geq3$ flies, $n\geq66$ ovarioles. n.s., not significant. Data are mean±s.d.

Development (2021) 148, dev199630. doi:10.1242/dev.199630

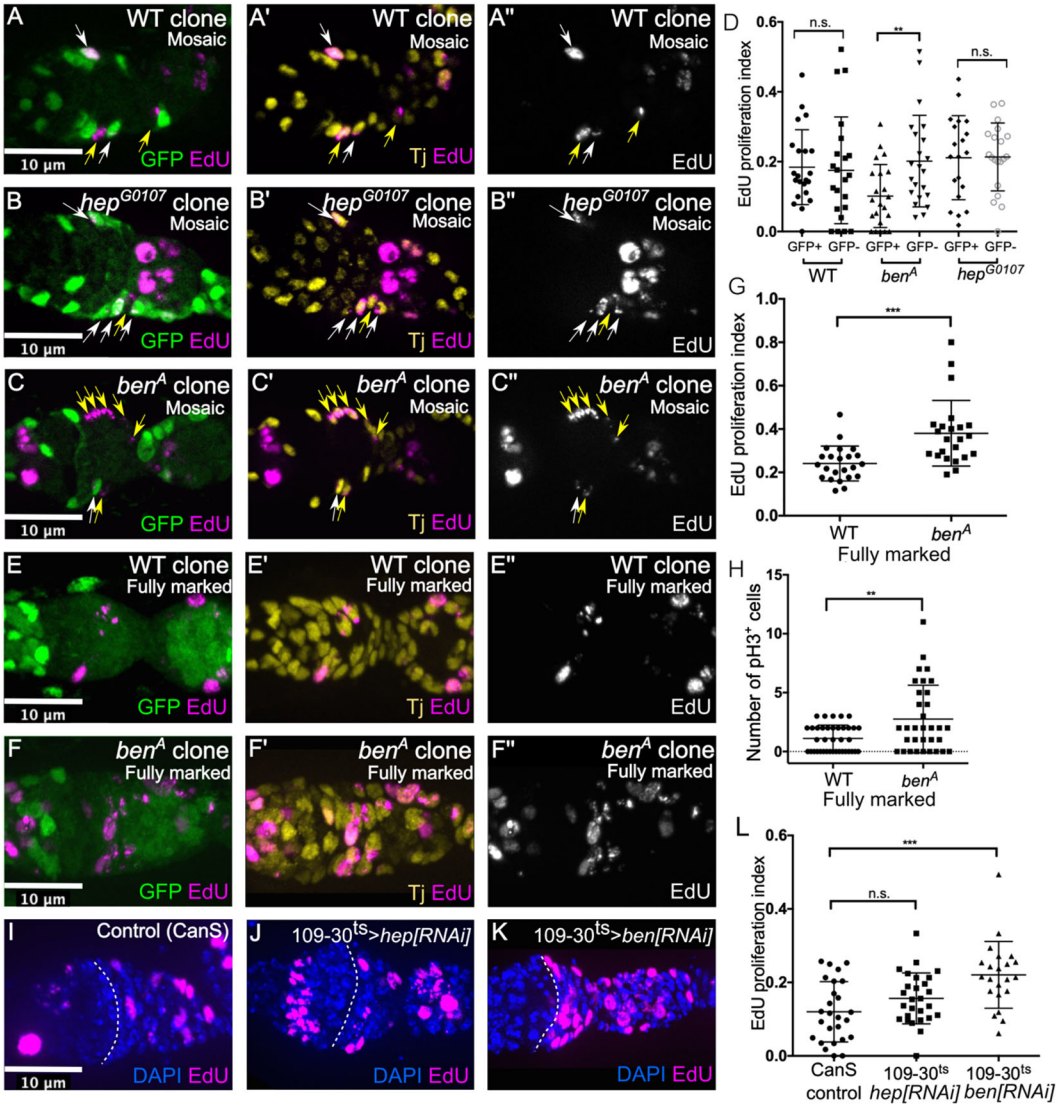

Fig. 7. Loss of *ben*, but not *hep*, causes increased proliferation in pFCs. (A-C″) Mosaic ovarioles with wild-type (WT), hep^{G0107} or ben^{A} clones stained for EdU incorporation (magenta) to identify cells in S-phase, the GFP clonal label (green) and Tj (yellow). Mosaic ovarioles contain both GFP^{+} (white arrows) and GFP^{-} (yellow arrows) cells. (D) Quantification of the EdU proliferation index in GFP^{+} and GFP^{-} cells in mosaic ovarioles of the indicated genotypes. Unpaired, two-tailed Student's *t*-test: $^{**}P<0.01$, $n\geq20$ ovarioles. (E-F″) Ovarioles in which the follicle cell populations in the germarium are fully marked by the lack of GFP were stained for EdU incorporation (magenta), the GFP clonal label (green), and Tj (yellow). (G,H) Quantification of the EdU proliferation index (G) and the number of $pH3^{+}$ follicle cells in germaria with fully marked wild-type or ben^{A} follicle cell populations (H). Unpaired, two-tailed Student's *t*-test: $^{**}P<0.01$, $^{***}P<0.001$, $n\geq23$ ovarioles. (I-K) Maximum intensity projection of ovarioles from Canton-S (CanS) flies (I) or *109-30^{ts}* driving *hep[RNAi]* or *ben[RNAi]* (J,K) stained for EdU incorporation (magenta) and DAPI (blue). Dashed white lines indicate the Region 2a/2b boundary. (L) Quantification of the EdU proliferation index in the indicated genotypes. Unpaired, two-tailed Student's *t*-test: $^{***}P<0.001$, $n\geq22$ ovarioles. n.s., not significant. Data are mean±s.d.

in promoting differentiation and proliferation in the early FSC lineage.

First, our findings demonstrate that *ben* functions along with the rest of the JNK signaling pathway to promote pFC differentiation. The phenotypes we observed in JNK pathway mutants strongly suggest that the primary defect is a failure to differentiate into mature stalk cells. The range of tube-like and expanded stalk morphological phenotypes we observed could both be explained by an inability of cells in the stalk regions between follicles to facilitate the pinching off of follicles from the germarium or to intercalate into a single row after the pinching off process has been initiated. We cannot rule out the possibility that differentiation toward the polar cell fate or main body cell fate are also impaired upon loss of JNK signaling, but we saw no evidence for this with the markers we used. Notably, although RNAi knockdown of *ben* or *hep* impaired the activity of a reporter for Notch signaling, *NRE-GFP*, in Region 2b pFCs and mature polar cells, this did not appear to interfere with the ability of mutant pFCs to differentiate into polar cells, so the significance of this effect on cell fate specification is unclear. Additional reporters of Notch signaling may help to determine the extent to which Notch signaling is disrupted in these mutant conditions. We also found that pERK is retained in pFCs of ovarioles with impaired JNK signaling, and that constitutive activation of pERK phenocopies the differentiation defects we observed in JNK pathway mutants. These observations suggest that JNK signaling promotes pFC differentiation into stalk cells by inhibiting the activation of ERK in pFCs.

Second, *ben* functions in a JNK-independent manner to help shape the gradient of Hh signaling in FSCs and pFCs. Indeed, we

Development (2021) 148, dev199630. doi:10.1242/dev.199630

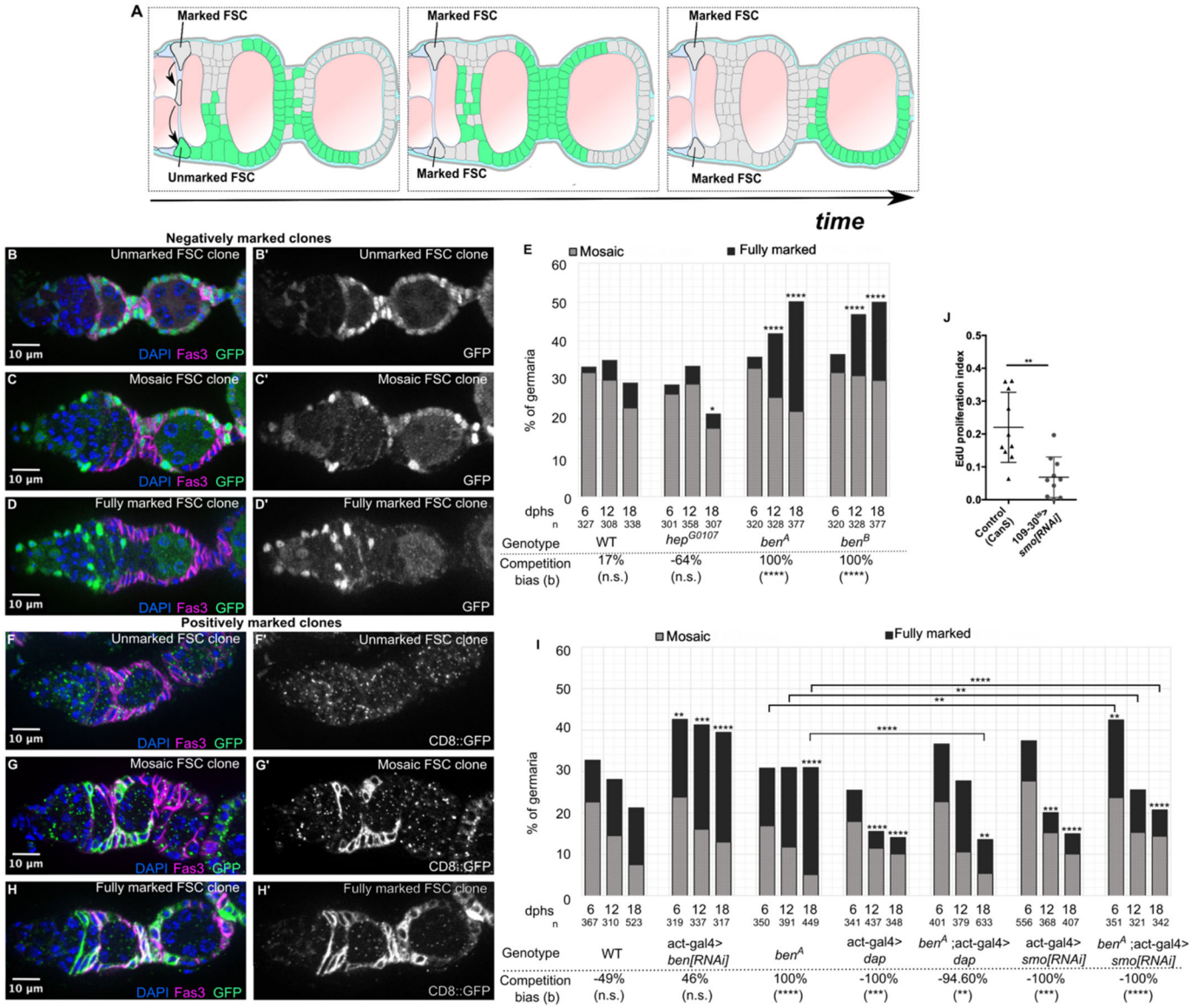

Fig. 8. Hypercompetition in *ben* mutant clones is suppressed by inhibition of proliferation or Hh signaling. (A) Schematic of FSC replacement through niche competition. (B-D′) Ovarioles that either lack GFP$^-$ clones (fully unmarked, B), contain both GFP$^+$ and GFP$^-$ follicle cells and thus are mosaic (C) or contain a follicle cell population that is fully GFP$^-$ (fully marked, D) stained for GFP (green), Fas3 (magenta) and DAPI (blue). (E) Quantification of ovarioles with a mosaic or fully-marked clone pattern at 6, 12 and 18 days post heat shock (dphs) of the indicated genotypes. (F-H′) Ovarioles with follicle cell populations that are unmarked (G), mosaic (H) and fully marked (I) with the GFP$^+$-marked clonal marking system, MARCM, stained for GFP (green), Fas3 (magenta) and DAPI (blue). (I) Quantification of ovarioles with a mosaic or fully-marked clone pattern at 6, 12 and 18 dphs of the indicated genotypes. In panels E and I, the competition bias (*b*) for the indicated genotypes, significance values for *b*, and the number of germaria scored (*n*) are shown below the graphs. Non-significant (n.s.) test statistics between conditions are not shown. Chi-squared test: **P*<0.05, ***P*<0.01, ****P*<0.001, *****P*<0.0001 (significance of results when compared with WT control ovarioles). (J) Quantification of EdU proliferation index in ovarioles from Canton-S (CanS) flies or with *109-30^{ts}* driving expression of *smo[RNAi]*. Unpaired, two-tailed Student's *t*-test: ***P*<0.01, *n*=10 ovarioles. Data are mean±s.d.

found that levels of *Ptc-pelican-GFP*, indicative of Hh signaling, are higher in *ben* mutant FSCs compared with wild type, and the *Ptc-pelican-GFP* reporter remains detectable throughout Regions 2b and 3 of the germarium. Likewise, we found that RNAi knockdown of *ben* caused the main body follicle cells to retain *zfh1* expression, a downstream target of Hh signaling, throughout the germarium and even into Stage 2 in some cases, where it is completely absent in wild-type tissue. However, we also found that *ben* mutant main body follicle cells were able to mature into a Cas$^+$, Eya$^-$ state, indicating proper differentiation with respect to these two markers. Thus, although loss of *ben* does not fully impair main body follicle cell differentiation, it may influence the process through its role as an upstream regulator of *zfh1* expression. Further study will be required to understand the functional significance of decreased *cas* and *zfh1* expression during main body follicle cell differentiation.

JNK signaling has been found to be involved in a wide variety of biological processes in a cell type- and context-dependent manner. Some of the most well-known functions of JNK signaling involve responses to non-homeostatic conditions, such as stress, cellular damage, infection and tumor growth (La Marca and Richardson, 2020; Pinal et al., 2019; Tafesh-Edwards and Eleftherianos, 2020). However, JNK signaling has also been found to be important for processes that occur during normal development or adult homeostasis (Hayes and Solon, 2017; Semba et al., 2020).

Development (2021) 148, dev199630. doi:10.1242/dev.199630

Indeed, *hep* mutants were originally described for their role in dorsal closure of the epidermis in the embryo (Glise et al., 1995), and subsequent studies have clearly established the importance of the JNK signaling pathway in this process (Hayes and Solon, 2017; Hou et al., 1997; Kockel et al., 1997; Kushnir et al., 2017; Riesgo-Escovar and Hafen, 1997). Likewise, JNK signaling is also important during adult homeostasis in mammalian stem cell lineages, for example to promote self-renewal of human hematopoietic stem cells (Xiao et al., 2019) and differentiation in the mouse intestinal stem cell and human neural stem cell lineages (Bengoa-Vergniory et al., 2014; Sancho et al., 2009). In line with this type of role for JNK signaling, our findings reveal new pathway interactions for JNK signaling in the regulation of cell fate decisions in an epithelial stem cell lineage.

In addition to regulating cell fate decisions, we also identified a JNK-independent role for Ben in the regulation of proliferation rate and FSC niche competition. Previous studies have established that increased proliferation causes hypercompetition (Wang et al., 2012), and that the proliferative response to Hh signaling is the key mediator of the FSC niche competition phenotypes in Hh pathway mutants (Huang and Kalderon, 2014). Therefore, the hypercompetition phenotype of *ben* mutant clones is likely caused, in large part, by the increased Hh signaling levels and proliferation rates in these mutants. Our findings that overexpression of *dap* or RNAi knockdown of *smo* was sufficient to suppress the hypercompetition phenotype of ben^{A} mutant clones are consistent with this. It is possible that delayed differentiation in newly-produced *ben* mutant pFCs also contributes to the hypercompetition phenotype. However, our observation that hep^{G0107} mutant clones are not hypercompetitive indicates that the hypercompetition phenotype of *ben* mutant clones is not caused by a block in the JNK-dependent functions of Ben in pFC differentiation.

Taken together, our findings indicate that Ben has JNK-dependent and -independent roles in regulating pFC cell fate decisions as they differentiate into polar, stalk and main body follicle cells. Specifically, our findings support a model (Fig. 9) in which JNK signaling promotes the differentiation of pFCs during normal homeostasis by helping to downregulate EGFR signaling in early pFCs. Previous studies found that pERK inhibits Groucho and that Groucho is required for the upregulation of Notch signaling in pFCs (Johnston et al., 2016). Thus, the retention of pERK in pFCs may explain why Notch signaling is not upregulated in JNK pathway mutants. Separately, Ben inhibits Hh signaling in a JNK-independent manner, thereby controlling pFC proliferation, regulating FSC niche competition, and possibly contributing to main body follicle cell differentiation. Thus, we have revealed a new layer of regulation within the signaling network that controls cell behavior in the early FSC lineage. The recently published single-cell atlases of the adult *Drosophila* ovary (Jevitt et al., 2020; Li et al., 2021 preprint; Rust et al., 2020; Slaidina et al., 2021a) revealed a continuum of changes in gene expression that occur during cellular differentiation in the early FSC lineage, and provide the tools for characterizing this signaling network in a cell-type specific manner. In future studies, it will be interesting to apply these new single-cell approaches to mutants such as those described here to further elucidate the molecular basis of cell fate decisions in the FSC lineage.

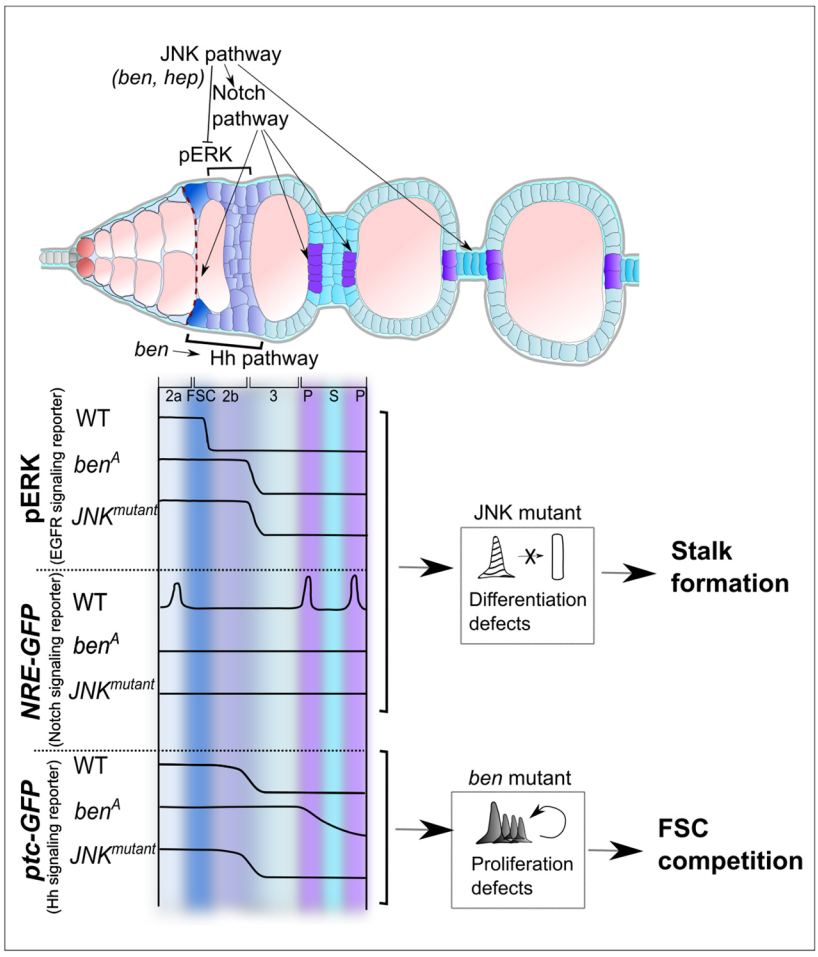

Fig. 9. Summary of the functions of Ben and JNK pathway genes in the FSC lineage. Ben positively regulates JNK signaling in the FSC lineage. JNK signaling downregulates the EGFR signaling reporter pERK and may promote Notch signaling in pFCs. In a JNK-independent manner, *ben* downregulates Hh signaling in pFCs. Schematics depict signaling pathway activity profiles in region 2a (2a), FSCs, Region 2b (2b), region 3 (3), polar (P) and stalk (S) cells in the FSC lineage. In schematics for each genotype, an increase or decrease in reporter signal (black line) is represented. pERK is detectable in ECs in Region 2a and FSCs at the 2a/b border, but is undetectable in early pFCs. *NRE-GFP*, a reporter for Notch signaling, is first detected along the 2a/b border, and then detected in mature polar cell clusters. *Ptc-pelican-GFP*, a reporter for Hh signaling activity, gradually decreases from ECs in Region 2a to early pFCs in Region 2b. Loss of JNK signaling leads to delays in differentiation and results in pFC differentiation defects. Loss of *ben* also leads to perdurance of Hh signaling beyond region 2b contributing to defects in differentiation and proliferation. Increased proliferation in *ben* mutants leads to FSC hypercompetition.

Development (2021) 148, dev199630. doi:10.1242/dev.199630

MATERIALS AND METHODS

Fly husbandry and stocks

All fly stocks were maintained on standard molasses food at 25°C. For experiments with flies that have *tub-Gal80^{ts}*, the crosses were performed at 18°C and adults were shifted to 29°C for 14 days, unless specified otherwise. For experiments with clones, flies were dissected at 12 days post clone induction, unless specified otherwise. Flies were obtained from Bloomington *Drosophila* Stock Center (BDSC), Vienna *Drosophila* Resource Center (VDRC) or Kyoto Stock Center (Kyoto), as indicated below.

IsoFRT19A (BDSC #1744); *ben^{A}, FRT19A* (BDSC #57057); *hsFlp, Ubi-GFP, FRT19A; 109-30-Gal4, tub-gal80^{ts}* (generated from BDSC #7019 and #7023); *UAS-ben[RNAi]* (VDRC #109638); *AP-1-GFP* kindly provided by the Hariharan Lab, University of California, Berkeley, USA (Chatterjee and Bohmann, 2012; Harris et al., 2016); *hsFlp, Ubi-RFP, FRT19A* (BDSC #31418); *UAS-hep[RNAi]* (VDRC #109277); *NRE-pGR* (Housden et al., 2012), referred to as NRE-GFP; *hep^{G0107}, FRT19A* (Kyoto #111740); *UAS-egr[RNAi]* (VDRC #108814); *UAS-grnd[RNAi]* (VDRC #104538); *UAS-traf6[RNAi]* (VDRC #110266); *Canton-S; UAS-ERK^{SEM}* (VDRC #59006); *w*; Ptc-pelican-GFP* generated in and kindly provided by the Kornberg lab, University of California, San Francisco, USA (Sahai-Hernandez and Nystul, 2013); *w*; UAS-Hh::eGFP/CyO* (BDSC #81024); *UAS-dap* kindly provided by the Buttitta lab, University of Michigan, USA (Lane et al., 1996); *hsFlp, tub-Gal80, FRT19A; Act5C-Gal4, UAS-CD8-GFP* (generated from BDSC #42726 and #44407); *UAS-smo[RNAi]* (BDSC #27037); *ben^{B}* (BDSC #57058); *UAS-bsk[RNAi]* (VDRC #104569); *10X-STAT-GFP* (BDSC #26197); *stl-Gal4* (BDSC #77732).

Immunostaining and imaging

Flies were dissected in 1× PBS at room temperature, samples were fixed for 15 min in 1× PBS with 4% paraformaldehyde and then rinsed twice with 1× PBS. Samples were blocked for 1 h at room temperature in block solution [1× PBS containing 0.2% Triton X-100 (PBST) and 0.5% bovine serum albumin (BSA)]. Samples were incubated overnight at 4°C with primary antibody diluted in block solution. Next, samples were rinsed twice and then incubated for 1 h at room temperature with block solution. Samples were incubated overnight at 4°C with secondary antibody diluted in block solution. Next, samples were rinsed twice with 1× PBST and then rinsed once with 1× PBS. Samples were mounted in DAPI Fluoromount-G (Thermo Fisher Scientific, OB010020).

The following primary antibodies were used: mouse anti-Fas3 [1:50; Developmental Studies Hybridoma Bank (DSHB), 7G10], guinea pig anti-GFP (1:1000; Synaptic Systems, 132005), guinea pig anti-Zfh1 (1:500; a gift from James Skeath, Washington University, St Louis, MO, USA), rabbit anti-GFP (1:1000; Torrey Pines Biolabs, TP-401), mouse anti-Eya (1:50; DSHB, 10H6), rabbit anti-Castor (1:5000; a gift from Ward Odenwald and Jonathan Benito Sipos, Universidad Autónoma de Madrid, Spain), rat anti-RFP (1:1000; ChromoTek, 5F8), rabbit anti-pERK (1:100; Cell Signaling Technology, 4370), guinea pig anti-Traffic Jam (1:5000, a gift from Dorothea Godt, University of Toronto, Canada), rabbit anti-Bazooka (Baz, 1:1000, a gift from Andreas Wodarz, Universitat Gottingen, Germany), rat anti-DE-Cadherin (Shotgun, 1:100, DSHB, DCAD2) and mouse anti-Discs Large (Dlg, 1:200, DSHB, 4F3). The following secondary antibodies were purchased from Thermo Fisher Scientific and used at 1:1000: goat anti-guinea pig 488 (A-11073), goat anti-guinea pig 633 (A-21450), goat anti-rabbit 488 (A-11008), goat anti-rabbit 555 (A-21428), goat anti-mouse 488 (A-11029), goat anti-mouse 555 (A-21424), goat anti-mouse 647 (A-21236), goat anti-mouse 555 (A-21236) and goat anti-rat 555 (A-21434).

Samples were imaged using a Zeiss M2 Axioimager with Apotome unit, Nikon C1si Spectral Confocal microscope or SP5 line-scanning confocal microscope. Image processing was carried out using FIJI and Inkscape.

EdU staining

For EdU assays, ovaries were dissected in 1× PBS and incubated in 1× PBS containing 15 µM EdU (Click-it EdU Alexa Fluor 555 Imaging Kit, Life Technologies, C10338) at room temperature for 1 h. Samples were rinsed twice with 1× PBS and fixed in 4% paraformaldehyde for 15 min. To permeabilize samples, ovaries were washed twice in 1× block (0.5% BSA in PBST) and incubated in fresh block solution for 1 h at room temperature. Then, samples were incubated overnight at 4°C with primary antibody solution. Next, samples were washed twice in 1× block for 10 min then incubated in a Click-iT reaction cocktail (1× Click-iT EdU reaction buffer, $CuSO_4$, 555-Alexa Fluor azide, 1× Click-iT EdU buffer additive) for 30 min at room temperature, protected from light. Samples were rinsed twice with 1× block then washed for 1 h in fresh block solution at room temperature. Samples were incubated overnight at 4°C in secondary antibody solution. Finally, samples were rinsed with 1× PBS and mounted using DAPI Fluoromount-G.

EdU proliferation index analysis

Images of ovarioles stained with Traffic Jam (Tj), a marker for somatic cell nuclei, and EdU, a marker for cells in S-phase, were analyzed using Imaris, as described previously (Fadiga and Nystul, 2019). Briefly, the Tj channel was processed for background subtraction, the surfaces tool was used to segment the images, and surfaces were used to quantify cell number and signal intensities. In mosaic clones, we determined the number of GFP^{+} and GFP^{-} cells, by measuring the intensity of GFP within each surface, determining the threshold of GFP intensity that distinguishes GFP^{+} cells from GFP^{-} cells, as determined by visual inspection of the image sets, and quantifying the number of surfaces above and below the threshold. The mean intensity of the EdU signal in each surface was then used to identify EdU^{+} cells. The EdU proliferation index was calculated by determining the ratio of the total number of EdU^{+} cells to the total number of cells in Region 2b. In mosaics, the total number of surfaces in Region 2b pertains to the total number of GFP^{+} or GFP^{-} cells in Region 2b.

Hybridization chain reaction

Probe sets of 20 probes per gene were custom made by Molecular Instruments. For *ben*, a sequence (X:13991931..14005990 from release 6.37) that is shared by all isoforms was submitted. For *hep*, the sequence of the hep-RA isoform (accession #NM_167346, FlyBase) was used. Before dissections, experimental flies were fed with molasses food and wet yeast for at least 3 consecutive days. The HCR protocol (Choi et al., 2018) was adapted for use in *Drosophila* ovaries, as described previously (Slaidina et al., 2021a,b). On the first day, fly ovaries were dissected in DPBS (CaCl, MgCl free) on ice. Samples were fixed in solution containing DPBS, 0.1% Tween and 4% paraformaldehyde for 20 min at room temperature. All subsequent steps were carried out in RNase free conditions, using reagents specified and supplied from the Molecular Instruments HCR v3.0 kit. Samples were permeabilized by rinsing twice with wash solution containing DPBS and 0.1% Tween at room temperature. Samples were then dehydrated on ice with sequential 20 min washes with solutions containing 25%, 50%, 75% and 100% methanol diluted in DPBS (in the order specified). The wash with 100% methanol was carried out twice. The samples were then stored overnight at −20°C. On the second day, samples were re-hydrated on ice with 20 min sequential washes with solutions containing 100%, 75%, 50%, 25% and 0% methanol in DPBS (in the order specified). Samples were washed for 2 h with a DPBS solution with 1% Triton-X. Then, samples were fixed in a solution containing DPBS, 0.1% Tween and 4% paraformaldehyde for 20 min at room temperature. Samples were washed for 5 min with wash solution (DPBS containing 0.1% Tween) twice on ice. Then, the samples were transferred to RNA-ase free Eppendorf tubes and incubated in a probe hybridization solution (containing a pre-warmed probe hybridization buffer mixed with 4-8 pmol of probe sets) for 24 h at 37°C. On the third day, samples underwent four 15-min washes with probe wash buffer solution. Samples were washed for 5 min with 5× SSCT at room temperature, followed by a 5 min incubation in pre-amplification buffer. Then, samples were incubated in light protected conditions for 16 h at room temperature in a hairpin solution (prepared by diluting snap-cooled hairpins in the pre-amplification buffer). On the next day, samples were washed twice for 5 min, twice for 30 min and lastly for 5 min with 5× SSCT. Then, DAPI Fluoromount-G was added and samples were mounted for imaging and analysis.

Clone induction

Newly eclosed adults of appropriate genotypes were collected and transferred to empty vials and capped with cotton balls (instead of vial

plugs). Flies were heat shocked by submerging vials into a 37°C water bath for 50 min to 1 h. Vials were removed and flies were transferred into vials with wet yeast and allowed to recover at room temperature for at least 6 h. This process was repeated twice, on two consecutive days. Flies were then incubated at 25°C and fed wet yeast daily. Flies were fed daily for at least 2 days preceding all experiments involving dissections.

FSC competition assay

Negatively marked clones and positively marked MARCM clones were generated using the clone induction protocol described above. The clone induction protocol resulted in germaria with fully marked, mosaic or unmarked stem cell clones. The frequency of clones in each of these categories was measured at 6, 12, and 18 days post clone induction (counted from the second day of heat shock). Over time, mosaic germaria can either become unmarked germaria or fully marked clones, indicating that stem cell replacement has occurred. An increase in the proportion of fully marked germaria is related to the rate of clone expansion, whereas an increase in the proportion of unmarked germaria is related to the rate of clone extinction. In wild-type tissue, the rates of extinction and expansion are approximately equal. Homozygosity for a mutation that promotes FSC retention in the niche or self-renewal will cause the rate of clonal expansion to be higher than the rate of clone extinction, resulting in FSC hypercompetition. Competition bias, *b*, was calculated as described previously (Kronen et al., 2014).

Statistics and graphs

Student's *t*-tests and Pearson's Chi-squared tests were used to calculate 95% confidence intervals and determine *P*-values using GraphPad Prism 6. Competition bias values, *b*, along with associated *P*-values, were calculated as previously described in Kronen et al. (2014). Bias was calculated using a MatLab script (Kronen et al., 2014). Comparisons between genotypes at individual time points were carried out using a Pearson's Chi-squared test in R. In all stacked graphs, cumulative percentages of indicated phenotypes have been represented. In bar graphs, individual dots represent percentages of phenotypes in each fly examined, and the bar height represents the mean percent of indicated phenotypes across replicates. The error bars shown in graphs represent standard deviation. Standard deviation was not calculated for Chi-squared tests. Multiple flies (*N*) were examined for each experiment and the ovariole number (*n*) equals the total number of ovarioles observed from all flies. No data points were excluded. Samples were not randomized or blinded. Raw data for all the quantifications have been provided in Table S1.

Acknowledgements

We are grateful to the Bloomington *Drosophila* Stock Center, Vienna *Drosophila* Resource Center and the Kyoto Stock Center, for stocks and reagents provided by Dr Ishwar Hariharan, Dr Thomas Kornberg, Dr James Skeath, Dr Andreas Wodarz, Dr Jonathan Benito Sipos, Dr Dorothea Godt, Dr Ward Odenwald and Dr Laura Buttitta, and for the HCR protocol provided by Dr Maija Slaidina and Dr Ruth Lehmann. We are thankful for the well-curated and very helpful resource, FlyBase. We sincerely thank Dr Katja Rust for her continual scientific advice throughout the project. We also thank Joshua Kim for his contributions to our finding that JNK signaling plays a role in follicle cell differentiation. Lastly, we thank all the members of the Nystul lab for helpful discussions, and Dr Katja Rust and Nathaniel Meyer for critical comments on the manuscript.

Competing interests

The authors declare no competing or financial interests.

Author contributions

Conceptualization: S.T., J.P., T.N.; Methodology: S.T., J.P., T.N.; Validation: S.T., J.P., T.N.; Formal analysis: S.T., J.P., T.N.; Investigation: S.T., J.P., T.N.; Resources: T.N.; Data curation: S.T., J.P., T.N.; Writing - original draft: S.T., J.P., T.N.; Writing - review & editing: S.T., J.P., T.N.; Visualization: S.T., J.P.; Supervision: S.T., T.N.; Project administration: S.T., T.N.; Funding acquisition: T.N.

Funding

This work was supported by grants from the National Institutes of Health (GM097158 including diversity supplement GM097158B for J.P. and GM136348). Deposited in PMC for release after 12 months.

Peer review history

The peer review history is available online at https://journals.biologists.com/dev/article-lookup/doi/10.1242/dev.199603

References

Assa-Kunik, E., Torres, I. L., Schejter, E. D., Johnston, D. S. and Shilo, B.-Z. (2007). Drosophila follicle cells are patterned by multiple levels of Notch signaling and antagonism between the Notch and JAK/STAT pathways. *Development* **134**, 1161-1169. doi:10.1242/dev.02800

Bach, E. A., Ekas, L. A., Ayala-Camargo, A., Flaherty, M. S., Lee, H., Perrimon, N. and Baeg, G.-H. (2007). GFP reporters detect the activation of the Drosophila JAK/STAT pathway in vivo. *Gene Expr. Patterns* **7**, 323-331. doi:10.1016/j.modgep.2006.08.003

Bai, J. and Montell, D. (2002). Eyes absent, a key repressor of polar cell fate during Drosophila oogenesis. *Development* **129**, 5377-5388. doi:10.1242/dev.00115

Baril, C., Sahmi, M., Ashton-Beaucage, D., Stronach, B. and Therrien, M. (2009). The PP2C Alphabet is a negative regulator of stress-activated protein kinase signaling in Drosophila. *Genetics* **181**, 567-579. doi:10.1534/genetics.108.096461

Bengoa-Vergniory, N., Gorroño-Etxebarria, I., González-Salazar, I. and Kypta, R. M. (2014). A switch from canonical to noncanonical Wnt signaling mediates early differentiation of human neural stem cells. *Stem Cells* **32**, 3196-3208. doi:10.1002/stem.1807

Berns, N., Woichansky, I., Friedrichsen, S., Kraft, N. and Riechmann, V. (2014). A genome-scale in vivo RNAi analysis of epithelial development in Drosophila identifies new proliferation domains outside of the stem cell niche. *J. Cell Sci.* **127**, 2736-2748. doi:10.1242/jcs.144519

Carpenter, A. T. C. (1975). Electron microscopy of meiosis in Drosophila melanogaster females. *Chromosoma* **51**, 157-182. doi:10.1007/BF00319833

Castanieto, A., Johnston, M. J. and Nystul, T. G. (2014). EGFR signaling promotes self-renewal through the establishment of cell polarity in Drosophila follicle stem cells. *eLife* **3**, e04437. doi:10.7554/eLife.04437

Chang, Y.-C., Jang, A. C.-C., Lin, C.-H. and Montell, D. J. (2013). Castor is required for Hedgehog-dependent cell-fate specification and follicle stem cell maintenance in Drosophila oogenesis. *Proc. Natl. Acad. Sci. USA* **110**, E1734-E1742. doi:10.1073/pnas.1300725110

Chatterjee, N. and Bohmann, D. (2012). A versatile ΦC31 based reporter system for measuring AP-1 and Nrf2 signaling in Drosophila and in tissue culture. *PLoS ONE* **7**, e34063. doi:10.1371/journal.pone.0034063

Choi, H. M. T., Schwarzkopf, M., Fornace, M. E., Acharya, A., Artavanis, G., Stegmaier, J., Cunha, A. and Pierce, N. A. (2018). Third-generation in situ hybridization chain reaction: multiplexed, quantitative, sensitive, versatile, robust. *Development* **145**, dev165753. doi:10.1242/dev.165753

Clayton, E., Doupé, D. P., Klein, A. M., Winton, D. J., Simons, B. D. and Jones, P. H. (2007). A single type of progenitor cell maintains normal epidermis. *Nature* **446**, 185-189. doi:10.1038/nature05574

Cook, M. S., Cazin, C., Amoyel, M., Yamamoto, S., Bach, E. and Nystul, T. (2017). Neutral competition for Drosophila follicle and cyst stem cell niches requires vesicle trafficking genes. *Genetics* **206**, 1417-1428. doi:10.1534/genetics.117.201202

Dai, W., Peterson, A., Kenney, T., Burrous, H. and Montell, D. J. (2017). Quantitative microscopy of the Drosophila ovary shows multiple niche signals specify progenitor cell fate. *Nat. Commun.* **8**, 1244. doi:10.1038/s41467-017-01322-9

Fadiga, J. and Nystul, T. G. (2019). The follicle epithelium in the Drosophila ovary is maintained by a small number of stem cells. *eLife* **8**, e49050. doi:10.7554/eLife.49050

Fox, D. T., Morris, L. X., Nystul, T. and Spradling, A. C. (2008). *StemBook*. Cambridge, MA: Harvard Stem Cell Institute.

Glise, B., Bourbon, H. and Noselli, S. (1995). hemipterous encodes a novel Drosophila MAP kinase kinase, required for epithelial cell sheet movement. *Cell* **83**, 451-461. doi:10.1016/0092-8674(95)90123-X

Guichard, A., Park, J. M., Cruz-Moreno, B., Karin, M. and Bier, E. (2006). Anthrax lethal factor and edema factor act on conserved targets in Drosophila. *Proc. Natl. Acad. Sci. USA* **103**, 3244-3249. doi:10.1073/pnas.0510748103

Hafezi, Y. and Nystul, T. G. (2001). Advanced techniques for cell lineage labelling in Drosophila. *eLS*. doi:10.1002/9780470015902.a0022539

Harris, R. E., Setiawan, L., Saul, J. and Hariharan, I. K. (2016). Localized epigenetic silencing of a damage-activated WNT enhancer limits regeneration in mature Drosophila imaginal discs. *eLife* **5**, e11588. doi:10.7554/eLife.11588

Hartman, T. R., Zinshteyn, D., Schofield, H. K., Nicolas, E., Okada, A. and O'Reilly, A. M. (2010). Drosophila Boi limits Hedgehog levels to suppress follicle stem cell proliferation. *J. Cell Biol.* **191**, 943-952. doi:10.1083/jcb.201007142

Hartman, T. R., Strochlic, T. I., Ji, Y., Zinshteyn, D. and O'Reilly, A. M. (2013). Diet controls Drosophila follicle stem cell proliferation via Hedgehog sequestration and release. *J. Cell Biol.* **201**, 741-757. doi:10.1083/jcb.201212094

Hayes, P. and Solon, J. (2017). Drosophila dorsal closure: an orchestra of forces to zip shut the embryo. *Mech. Dev.* **144**, 2-10. doi:10.1016/j.mod.2016.12.005

Herrera, S. C. and Bach, E. A. (2021). The emerging roles of JNK signaling in Drosophila stem cell homeostasis. *Int. J. Mol. Sci.* **22**, 5519. doi:10.3390/ijms22115519

Hou, X. S., Goldstein, E. S. and Perrimon, N. (1997). Drosophila Jun relays the Jun amino-terminal kinase signal transduction pathway to the Decapentaplegic signal transduction pathway in regulating epithelial cell sheet movement. *Genes Dev.* **11**, 1728-1737. doi:10.1101/gad.11.13.1728

Housden, B. E., Millen, K. and Bray, S. J. (2012). Drosophila reporter vectors compatible with ΦC31 integrase transgenesis techniques and their use to generate new notch reporter fly lines. *G3* **2**, 79-82. doi:10.1534/g3.111.001321

Huang, J. and Kalderon, D. (2014). Coupling of Hedgehog and Hippo pathways promotes stem cell maintenance by stimulating proliferation. *J. Cell Biol.* **205**, 325-338. doi:10.1083/jcb.201309141

Jevitt, A., Chatterjee, D., Xie, G., Wang, X.-F., Otwell, T., Huang, Y.-C. and Deng, W.-M. (2020). A single-cell atlas of adult Drosophila ovary identifies transcriptional programs and somatic cell lineage regulating oogenesis. *PLoS Biol.* **18**, e3000538. doi:10.1371/journal.pbio.3000538

Johnston, M. J., Bar-Cohen, S., Paroush, Z. and Nystul, T. G. (2016). Phosphorylated Groucho delays differentiation in the follicle stem cell lineage by providing a molecular memory of EGFR signaling in the niche. *Development* **143**, 4631-4642. doi:10.1242/dev.143263

Kim-Yip, R. P. and Nystul, T. G. (2018). Wingless promotes EGFR signaling in follicle stem cells to maintain self-renewal. *Development* **145**, dev168716. doi:10.1242/dev.168716

Klein, A. M. and Simons, B. D. (2011). Universal patterns of stem cell fate in cycling adult tissues. *Development* **138**, 3103-3111. doi:10.1242/dev.060103

Koch, E. A. and King, R. C. (1966). The origin and early differentiation of the egg chamber of Drosophila melanogaster. *J. Morphol.* **119**, 283-303. doi:10.1002/jmor.1051190303

Kockel, L., Zeitlinger, J., Staszewski, L. M., Mlodzik, M. and Bohmann, D. (1997). Jun in Drosophila development: redundant and nonredundant functions and regulation by two MAPK signal transduction pathways. *Genes Dev.* **11**, 1748-1758. doi:10.1101/gad.11.13.1748

Kronen, M. R., Schoenfelder, K. P., Klein, A. M. and Nystul, T. G. (2014). Basolateral junction proteins regulate competition for the follicle stem cell niche in the Drosophila ovary. *PLoS ONE* **9**, e101085. doi:10.1371/journal.pone.0101085

Kushnir, T., Mezuman, S., Bar-Cohen, S., Lange, R., Paroush, Z. and Helman, A. (2017). Novel interplay between JNK and Egfr signaling in Drosophila dorsal closure. *PLoS Genet.* **13**, e1006860. doi:10.1371/journal.pgen.1006860

La Marca, J. E. and Richardson, H. E. (2020). Two-faced: roles of JNK signalling during tumourigenesis in the Drosophila model. *Front. Cell Dev. Biol.* **8**, 42. doi:10.3389/fcell.2020.00042

Lane, M. E., Sauer, K., Wallace, K., Jan, Y. N., Lehner, C. F. and Vaessin, H. (1996). Dacapo, a cyclin-dependent kinase inhibitor, stops cell proliferation during Drosophila development. *Cell* **87**, 1225-1235. doi:10.1016/S0092-8674(00)81818-8

Lee, T. and Luo, L. (2001). Mosaic analysis with a repressible cell marker (MARCM) for Drosophila neural development. *Trends Neurosci.* **24**, 251-254. doi:10.1016/S0166-2236(00)01791-4

Li, H., Janssens, J., De Waegeneer, M., Kolluru, S. S., Davie, K., Gardeux, V., Saelens, W., David, F., Brbić, M., Leskovec, J. et al. (2021). Fly Cell Atlas: a single-cell transcriptomic atlas of the adult fruit fly. *bioRxiv*, 2021.07.04.451050.

Lopez-Schier, H. and St Johnston, D. (2001). Delta signaling from the germ line controls the proliferation and differentiation of the somatic follicle cells during Drosophila oogenesis. *Genes Dev.* **15**, 1393-1405. doi:10.1101/gad.200901

Ma, X., Li, W., Yu, H., Yang, Y., Li, M., Xue, L. and Xu, T. (2014). Bendless modulates JNK-mediated cell death and migration in Drosophila. *Cell Death Differ.* **21**, 407-415. doi:10.1038/cdd.2013.154

Margolis, J. and Spradling, A. (1995). Identification and behavior of epithelial stem cells in the Drosophila ovary. *Development* **121**, 3797-3807. doi:10.1242/dev.121.11.3797

McGuire, S. E., Le, P. T., Osborn, A. J., Matsumoto, K. and Davis, R. L. (2003). Spatiotemporal rescue of memory dysfunction in Drosophila. *Science* **302**, 1765-1768. doi:10.1126/science.1089035

Melamed, D. and Kalderon, D. (2020). Opposing JAK-STAT and Wnt signaling gradients define a stem cell domain by regulating differentiation at two borders. *eLife* **9**, e61204. doi:10.7554/eLife.61204

Michel, M., Kupinski, A. P., Raabe, I. and Bökel, C. (2012). Hh signalling is essential for somatic stem cell maintenance in the Drosophila testis niche. *Development* **139**, 2663-2669. doi:10.1242/dev.075242

Miller, A. (1950). The internal anatomy and histology of the imago of Drosophila melanogaster. In *Biology of Drosophila* (ed. M Demerec), pp. 421-534. Cold Spring Harbor Laboratory Press.

Nystul, T. G. and Spradling, A. (2007). An epithelial niche in the Drosophila ovary undergoes long-range stem cell replacement. *Cell Stem Cell* **1**, 277-285. doi:10.1016/j.stem.2007.07.009

Nystul, T. G. and Spradling, A. (2010). Regulation of epithelial stem cell replacement and follicle formation in the Drosophila ovary. *Genetics* **184**, 503-515. doi:10.1534/genetics.109.109538

Pinal, N., Calleja, M. and Morata, G. (2019). Pro-apoptotic and pro-proliferation functions of the JNK pathway of Drosophila: roles in cell competition, tumorigenesis and regeneration. *Open Biol.* **9**, 180256. doi:10.1098/rsob.180256

Riesgo-Escovar, J. R. and Hafen, E. (1997). Drosophila Jun kinase regulates expression of decapentaplegic via the ETS-domain protein Aop and the AP-1 transcription factor DJun during dorsal closure. *Genes Dev.* **11**, 1717-1727. doi:10.1101/gad.11.13.1717

Rust, K. and Nystul, T. (2020). Signal transduction in the early Drosophila follicle stem cell lineage. *Curr. Opin. Insect Sci.* **37**, 39-48. doi:10.1016/j.cois.2019.11.005

Rust, K., Byrnes, L. E., Yu, K. S., Park, J. S., Sneddon, J. B., Tward, A. D. and Nystul, T. G. (2020). A single-cell atlas and lineage analysis of the adult Drosophila ovary. *Nat. Commun.* **11**, 5628. doi:10.1038/s41467-020-19361-0

Sahai-Hernandez, P. and Nystul, T. G. (2013). A dynamic population of stromal cells contributes to the follicle stem cell niche in the Drosophila ovary. *Development* **140**, 4490-4498. doi:10.1242/dev.098558

Sancho, R., Nateri, A. S., de Vinuesa, A. G., Aguilera, C., Nye, E., Spencer-Dene, B. and Behrens, A. (2009). JNK signalling modulates intestinal homeostasis and tumourigenesis in mice. *EMBO J.* **28**, 1843-1854. doi:10.1038/emboj.2009.153

Semba, T., Sammons, R., Wang, X., Xie, X., Dalby, K. N. and Ueno, N. T. (2020). JNK signaling in stem cell self-renewal and differentiation. *Int. J. Mol. Sci.* **21**, 2613. doi:10.3390/ijms21072613

Singh, T., Lee, E. H., Hartman, T. R., Ruiz-Whalen, D. M. and O'Reilly, A. M. (2018). Opposing action of Hedgehog and insulin signaling balances proliferation and autophagy to determine follicle stem cell lifespan. *Dev. Cell* **46**, 720-734.e6. doi:10.1016/j.devcel.2018.08.008

Slaidina, M., Gupta, S. and Lehmann, R. (2021a). A single cell atlas reveals unanticipated cell type complexity in Drosophila ovaries. *bioRxiv*. doi:10.1101/2021.01.21.427703

Slaidina, M., Gupta, S., Banisch, T. U. and Lehmann, R. (2021b). A single-cell atlas reveals unanticipated cell type complexity in Drosophila ovaries. *Genome Res.* **31**, 1938-1951. doi:10.1101/gr.274340.120

Song, X. and Xie, T. (2003). Wingless signaling regulates the maintenance of ovarian somatic stem cells in Drosophila. *Development* **130**, 3259-3268. doi:10.1242/dev.00524

Tafesh-Edwards, G. and Eleftherianos, I. (2020). JNK signaling in Drosophila immunity and homeostasis. *Immunol. Lett.* **226**, 7-11. doi:10.1016/j.imlet.2020.06.017

Ulmschneider, B., Grillo-Hill, B. K., Benitez, M., Azimova, D. R., Barber, D. L. and Nystul, T. G. (2016). Increased intracellular pH is necessary for adult epithelial and embryonic stem cell differentiation. *J. Cell Biol.* **215**, 345-355. doi:10.1083/jcb.201606042

Vied, C., Reilein, A., Field, N. S. and Kalderon, D. (2012). Regulation of stem cells by intersecting gradients of long-range niche signals. *Dev. Cell* **23**, 836-848. doi:10.1016/j.devcel.2012.09.010

Wang, Z. A., Huang, J. and Kalderon, D. (2012). Drosophila follicle stem cells are regulated by proliferation and niche adhesion as well as mitochondria and ROS. *Nat. Commun.* **3**, 769. doi:10.1038/ncomms1765

Xiao, X., Lai, W., Xie, H., Liu, Y., Guo, W., Liu, Y., Li, Y., Li, Y., Zhang, J., Chen, W. et al. (2019). Targeting JNK pathway promotes human hematopoietic stem cell expansion. *Cell Discov.* **5**, 2. doi:10.1038/s41421-018-0072-8

Zhang, Y. and Kalderon, D. (2000). Regulation of cell proliferation and patterning in Drosophila oogenesis by Hedgehog signaling. *Development* **127**, 2165-2176. doi:10.1242/dev.127.10.2165

Zhang, Y. and Kalderon, D. (2001). Hedgehog acts as a somatic stem cell factor in the Drosophila ovary. *Nature* **410**, 599-604. doi:10.1038/35069099